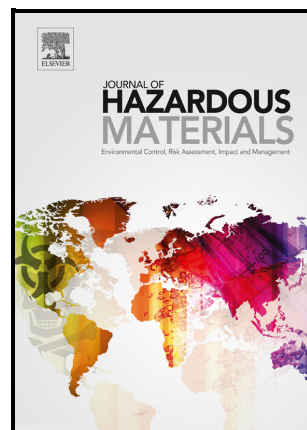


Attic dust: an archive of historical air contamination of the urban environment and potential hazard to health?

Martin GABERŠEK, Michael J. WATTS, Mateja GOSAR



PII: S0304-3894(22)00534-9

DOI: <https://doi.org/10.1016/j.jhazmat.2022.128745>

Reference: HAZMAT128745

To appear in: *Journal of Hazardous Materials*

Received date: 25 November 2021

Revised date: 25 February 2022

Accepted date: 17 March 2022

Please cite this article as: Martin GABERŠEK, Michael J. WATTS and Mateja GOSAR, Attic dust: an archive of historical air contamination of the urban environment and potential hazard to health?, *Journal of Hazardous Materials*, (2021) doi:<https://doi.org/10.1016/j.jhazmat.2022.128745>

This is a PDF file of an article that has undergone enhancements after acceptance, such as the addition of a cover page and metadata, and formatting for readability, but it is not yet the definitive version of record. This version will undergo additional copyediting, typesetting and review before it is published in its final form, but we are providing this version to give early visibility of the article. Please note that, during the production process, errors may be discovered which could affect the content, and all legal disclaimers that apply to the journal pertain.

© 2021 Published by Elsevier.

## **Attic dust: an archive of historical air contamination of the urban environment and potential hazard to health?**

Authors: Martin GABERŠEK <sup>a</sup>, Michael J. WATTS <sup>b</sup>, Mateja GOSAR <sup>a</sup>

<sup>a</sup> Geological Survey of Slovenia, Dimičeva ulica 14, SI-1000 Ljubljana, Slovenia  
(martin.gabersek@geo-zs.si; mateja.gosar@geo-zs.si)

<sup>b</sup>Inorganic Geochemistry, Centre for Environmental Geochemistry, British Geological Survey, Keyworth, Nottingham NG12 5GG, United Kingdom (mwatts@bgs.ac.uk)  
(corresponding author: martin.gabersek@geo-zs.si, +38612809765)

### **Abstract**

A comprehensive study of attic dust in an urban area is presented. Its entire life cycle, from determining historical emission sources to recognising the processes that take place in attic dust and its potential to impact human health is discussed. Its chemical composition and morphological characteristics of individual solid particles reflect past anthropogenic activities. High levels of Be-Cd-Cu-Sb-Sn-Pb-Te-Zn and occurrence of Cu-Zn shavings are typical for an industrial zone characterised by a foundry and a battery factory. High levels of Co-Fe-Mo-Ni-W-Ba-Cr-Mg-Mn-Nb-Ti and occurrence of various solid Fe-oxides, particularly spherical particles, were identified in another industrial zone, which was dominated by the automotive and metal-processing industries. Emissions from coal combustion affected the distribution of S-Se-Hg-Tl-As-Ag-U. The predominant mineral in attic dust is gypsum, which was presumably formed *in situ* by the reaction of carbonate dust particles and atmospheric SO<sub>2</sub> gas. The high oral bioaccessibility of As-Cd-Cu-Pb-Zn in the gastric phase and high bioaccessibility of As-Cu-Cd-Ni in the gastrointestinal phase were identified. Determined characteristics of attic dust and identified possibilities of prolonged human exposure to it indicate that attic dust should be treated as an excellent proxy for historical air contamination as well as a potentially hazardous material for human health.

**Key words:** multi-element composition, scanning electron microscopy, oral bioaccessibility, Unified BARGE method, urban geochemistry

## 1. Introduction

The anthropogenic contamination and pollution of the environment with potentially toxic elements (PTEs) is one of the major issues challenging the Anthropocene, a newly proposed human-dominated geological epoch (Lewis & Maslin, 2015). Although PTEs are naturally present in the environment, various anthropogenic activities significantly alter their natural biogeochemical cycles (Rauch & Pacyna, 2009; Selin, 2009; Lewis & Maslin, 2015; Herath et al., 2017). The impacts of humankind on global biogeochemical PTE cycles are so profound that some authors even suggest using the term “anthrobiogeochemical cycles” (Rauch & Pacyna, 2009; Mitra & Sen, 2017). For example, anthropogenic activities have increased the amount of mercury cycling between the land, atmosphere, and ocean by a factor of three to five (Selin, 2009). The negative impacts are even more pronounced at local levels, especially in highly urbanised areas. Due to the detrimental effects on the environment and human health, one of the most pressing issues connected with anthropogenic activities are emissions of particulate matter (PM), including PTE-bearing particles (Karagulian et al., 2015). Some of the biggest and most important anthropogenic sources are mining, metallurgical and industrial activities, combustion processes, transportation, and urbanisation (Thorpe & Harrison, 2008; Tack, 2010; Lyons & Harmon, 2012; Žibret et al., 2013; Karagulian et al., 2015; Žibret, 2018; Ali et al., 2019; Jabłońska & Janeczek, 2019; Miler & Gosar, 2019; Jeong et al., 2020; Miler, 2020; O’Shea et al., 2020; Teran et al., 2020; Gaberšek & Gosar, 2021a; Kelepertzis et al., 2021). In addition to anthropogenic sources, PM also originates from various natural sources and processes, such as soil erosion, volcanic activity, forest fires, and biological material (Calvo et al., 2013; Miler, 2014; Karagulian et al., 2015). Since PTEs are non-biodegradable and accumulative in nature (Wong et al., 2006), their presence in the environment is the result not only of ongoing anthropogenic activities, but also of historical ones. Which is why it is important to study the anthropogenic impact and extent of such on the environment in the past, to identify sources of PTEs, and try to separate past and present emissions sources.

Past anthropogenic emissions and contamination of the environment with PTEs can be assessed by studying various media. One such medium is attic dust, which is a type of dust that is deposited in uninhabited and uninsulated attics in which the disturbance by inhabitants of such is likely to be minimized (Cizdziel & Hodge, 2000; Šajin, 2003; Davis & Gulson, 2005; Gosar et al., 2006). This type of dust is also referred to as “ceiling dust” (Davis & Gulson, 2005) and “roof cavity dust” (Wheeler et al., 2020) in the scientific literature. Attic dust consists of airborne particulate matter originating mostly from natural and external anthropogenic sources. It enters attics through various cracks, gaps, and openings due to differences in air pressure, where the air pressure inside, in attics, is lower than it is outside (Cizdziel & Hodge, 2000; Davis & Gulson, 2005). Attic dust has several advantages over other media in the effort to reconstruct historical air contamination. The particulate matter accumulates and remains undisturbed in attics for decades, as it is not subject to the direct influence of any occupants’ activities or weather conditions, which means that the natural degradative processes catalysed by sunlight and rain are minimised or completely eliminated (Cizdziel & Hodge, 2000). Its main advantage over using lake sediment and glaciers to determine past contamination is its greater spatial flexibility (e.g. attic dust studies can be performed on far smaller scales than can studies of glaciers), more ubiquitous distribution and proximity to anthropogenic sources. Its main advantage over living organisms that are used for the same purposes (e.g. trees) is the fact that organisms absorb chemical species selectively and sometimes serve to render them more concentrated (Ilacqua et al., 2003). The most important disadvantages of using attic dust as the subject of environmental geochemical studies are its limited use in sparsely populated areas and/or the limited number of appropriate attics, the specifics of contaminants in a particulate phase, and the integrated nature of related information (Ilacqua et al., 2003). Nevertheless, numerous studies have shown that the continuous, undisturbed deposition and enduring stability of attic dust over a long period of time allows for the indirect assessment of historical air contamination with PTEs and the determination of spatial as well as temporal patterns of related anthropogenic emissions going back to the time the building was constructed and up to the present day (Cizdziel & Hodge, 2000; Gosar & Šajin, 2001; Ilacqua et al., 2003; Šajin, 2003; Davis & Gulson, 2005; Gosar et al., 2006; Tye et al., 2006; Žibret,

2008; Coronas et al., 2013; Völgyesi et al., 2014; Baricza et al., 2016; Balabanova et al., 2017; Miler & Gosar, 2019; Van Pelt et al., 2020; Paineur et al., 2022). Only a few of these complemented their chemical analyses of attic dust using microscopic techniques (Tye et al., 2006; Baricza et al., 2016; Miler & Gosar, 2019). There are also very scarce data on particle distribution of attic dust. Cizdziel et al. (1998) determined that 50 mass% of the dust belongs to size fraction of  $<53 \mu\text{m}$ , while Davis & Gulson (2005) identified a bimodal distribution, and the volumes of fine dusts were 50%  $<63 \mu\text{m}$ , 30%  $<38 \mu\text{m}$ , and 7%  $<10 \mu\text{m}$ . Attic dust can also be used as a robust household-level exposure proxy to air contamination during extreme events such as fires (Wheeler et al., 2020). In addition to serving as an archive of historical air contamination, attic dust may also act as a source of recent contamination in cases of the renovation and demolition of old buildings, and can also pose a potential hazard to human health if it migrates through openings into inhabited parts of buildings (Davis & Gulson, 2005). Nevertheless, studies of the bioaccessibility of PTEs in attic dust are very rare. As far as we know, there has been only one such study (Bačeva-Andonovska et al., 2015).

The presented research is a part of a broader study of geochemistry of the urban environment. A part of the geochemical and SEM/EDS results given here has already been used for the comparison with other environmental media but without detailed interpretation provided (Gaberšek & Gosar, 2021b). The aim of the Gaberšek & Gosar (2021b) paper was to apply theoretical foundations of the holistic approach to the geochemistry of solid inorganic particles in an urban area by studying street, attic, and household dust and airborne PM. The similarities/differences of the studied urban media were determined and the importance of the holistic approach in urban areas was highlighted. One of the important outcomes of that research was identification of the uniqueness and usefulness of attic dust as a sampling medium which, however, could not be sufficiently discussed in the scope of Gaberšek & Gosar (2021b) paper. Therefore, the aim of the presented research was to provide detailed and comprehensive geochemical characterisation of attic dust in an urban area and to determine its entire life cycle: from the determination of its sources to recognition of the processes within attics and its potential hazard to human health. This aim was achieved by determining the multi-element chemical composition of attic dust, assessing its mineralogical composition, determining the morphological and

chemical characteristics of individual PTE-bearing particles in attic dust, and by determining the oral bioaccessibility of ten selected PTEs (As, Cd, Cr, Cu, Hg, Ni, Pb, Sb, Sn, and Zn). The results serve (1) to underline the value of examining attic dust in geochemical studies of urban areas and its usefulness in determining the historical anthropogenic impact of such on the environment (2) to emphasise its potential hazard to human health. Such a comprehensive study, the first of its kind, offers a new perspective on attic dust and may encourage new and innovative studies of the attic dust in the future.

## **2. Materials and Methods**

### **2.1 Study area**

The presented study of attic dust was performed in the town of Maribor, Slovenia (46°32' N, 15°39' E, 275 m above sea level (Fig. 1); 95,000 inhabitants). Maribor was an important industrial centre in the 20<sup>th</sup> century, with textile and metal industries as the most important industrial sectors. The industrial development of the area started with the construction of Vienna-Trieste railway in the mid-19<sup>th</sup> century and electrification of the town (construction of hydropower plants on the Drava River) at the beginning of the 20<sup>th</sup> century (Slavec, 1991; Oset, 2010). The following three industrial zones developed through the time: Studenci, Melje, and Tezno. The first large industrial plant in Maribor was the railway workshop designed for repairing railway carriages located in the Studenci industrial zone. The most important industrial sector between both world wars was the textile industry, followed by metal and chemical industries. After World War II, Maribor was subjected to the aggregation of smaller factories into large companies; typically employing several thousands of employees (Slavec, 1991). The metal industry took over the position of the most significant industrial sector. There were a large truck and bus factory (TAM) and crane factory (METALNA) in the Tezno industrial zone. The Melje industrial zone was dominated by a foundry (MLM), which has been producing forged semi-products out of copper alloys (e.g. bronze bells, brass rods), die-casting parts and different steel tools (it is still in operation but on a smaller scale), the largest textile factory in the whole Yugoslavia (MTT), a battery factory (VESNA), and a factory of detergents and personal hygiene products (HENKEL). Railway vehicle factory (TVT B. KIDRIČ) was located in the Studenci industrial zone.

There were also numerous smaller metal-processing plants throughout the town (e.g. metal furniture factory in Melje). The importance of industry has tapered off over the last 30–35 years owing to various political and economic factors. Nevertheless, it still plays an important role in the town's economy. Current industrial facilities are mainly concentrated in the Melje and Tezno industrial zones. The first is characterised by a foundry and a metal furniture factory. The automotive and metal processing factories as well as waste treatment plants are located in the Tezno industrial zone.

The climate of the area is continental with the average annual temperature of 10.5 °C (over the period 1981–2010) and the average precipitation of 1015 mm (Nadbath, 2019). The prevailing wind direction is from northwest and the average wind speed is 1.8 m/s (Bertalanič, 2007). The town of Maribor developed on the Drava River alluvial plain, which consists predominantly of metamorphic and igneous rock fragments (Mioč and Žnidarčič, 1989; Šoster et al., 2017; Mencin-Gale et al., 2019). The wider surroundings of the town are underlain by metamorphic and igneous rocks (SW and NW of the town) as well as siliciclastic rocks, unconsolidated sediments and, to a lesser extent, carbonate rocks (Mioč, 1978; Mioč & Žnidarčič, 1989). Detailed information on the climate, geological setting, and soil types in the wider surroundings of Maribor as well as data on its historical industrial development can be found in Gaberšek & Gosar (2018; 2021b).

## **2.2 Sampling and sample preparation**

The sampling of attic dusts was carried out in the summer of 2017, which was accomplished by brushing the dust off the surfaces of wooden building elements in uninhabited and uninsulated attics. One sample, consisting of at least 10 subsamples, was taken in each attic. At each sampling site, a new, clean nylon brush was used. Dust was brushed onto a white piece of paper and then packed in polyethylene bags. Samples were taken from 19 buildings (Fig. 1), most of which were more than 80 years old (the youngest three were built in the 1950s). Out of 19 buildings, 15 was located in the residential areas and 4 in the industrial areas (details are given in Appendix SM2 in the supplementary material). Past human disturbances of attics were not detected, with the exception of replacement of roof tiles at some sites which could disturb the settled dust. Spatial distribution of the sampling sites

was dependent on the availability of suitable attics and the willingness of the residents to take part in the study. Samples were oven-dried at 35 °C and sieved at <0.063 mm using nylon sieves. The coarse fraction was discarded and only the <0.063 mm fraction was studied.

### **2.3 Determination of chemical composition**

The chemical composition of all attic dust samples was determined by ICP-MS after a modified aqua regia digestion ( $\text{HCl}:\text{HNO}_3:\text{H}_2\text{O} = 1:1:1$ , at 95 °C). The mass of each sample was 0.5 g. Levels of the following 65 elements were determined: Ag, Al, As, Au, B, Ba, Be, Bi, Ca, Cd, Ce, Co, Cr, Cs, Cu, Dy, Er, Eu, Fe, Ga, Gd, Ge, Hf, Hg, Ho, In, K, La, Li, Lu, Mg, Mn, Mo, Na, Nb, Nd, Ni, P, Pb, Pd, Pr, Pt, Rb, Re, S, Sb, Sc, Se, Sm, Sn, Sr, Ta, Tb, Te, Th, Ti, Tl, Tm, U, V, W, Y, Yb, Zn, Zr. Total organic carbon (TOC) was determined using a LECO analyser in only 12 selected samples due to insufficient amounts of other samples. The individual mass of samples was 5 g. The analytical work was performed at Bureau Veritas Mineral Laboratories, Vancouver, Canada. The quality of analyses was ensured by randomising sample numbers and the inclusion of Certified Reference Materials (BCR 146R, OREAS 45D, OREAS 45E, OREAS 151 B) and replicates of five attic dust samples in the sample batch. Accuracy was estimated by calculating the relative error (RE; in %), and precision by calculating the Relative Percent Difference (RPD; in %). Elements for which more than 20% of the measurements were below their detection limits, calculated mean RE was >20% and/or mean RPD >30%, were excluded from further statistical treatment. These are: Au, Ge, Hf, In, Pd, Pt, Re, and Ta. Details are given in Appendix SM1 (Table S1) in the supplementary material.

### **2.4 Characterisation of the individual particles with SEM/EDS**

The detailed characterisation of the individual particles in attic dust using scanning electron microscope (SEM; JEOL JSM 6490LV) with energy dispersive spectroscopy (EDS; Oxford INCA PentaFET3 Si(Li) detector) followed a method established and described by Miler & Gosar (2013; 2015) and Gaberšek & Gosar (2021a; 2021b). The following four samples were analysed with the SEM/EDS: MBAD02 (old town centre), MBAD09 (newer residential area, close to the Tezno industrial zone), MBAD14 (Melje industrial zone), MBAD21 (Tezno industrial zone) (Fig. 1).

Samples were chosen based on their chemical composition (the two samples from industrial zones show elevated levels of some PTEs) and land use (two industrial and two residential). Five fields-of-view at a magnification of 300× were randomly selected for each sample. First, a surface EDS analysis (mapping) of each field was performed. The results served as the basis for an assessment of the relative mineral and other phase (e.g. organic matter, alloys) abundances. Next, a detailed semi-quantitative and qualitative analysis of all PTE-bearing particles in five fields-of-view was performed, using a Backscattered electron mode (BSE). The size (length of the longest axis), morphology and chemical composition of each PTE-bearing particle and other particles whose morphology (e.g. spheres, shavings) indicated their anthropogenic origin were determined. These are simply given as a combination of constituent elements. Those elements, whose concentrations are at least 10-times lower than the concentrations of the predominant element (according to the atomic percentages of the elements acquired with EDS) appear in brackets. Where appropriate, possible natural mineral equivalents of PTE-bearing particles are given. The analysed particles were classified into the following nine groups, which were established based on the results: *Fe-oxides* (consisting mainly of Fe and O), *Spherical Fe-oxides* (spherical particles consisting mainly of Fe and O), *Fe-alloys* (consisting mainly of Fe and smaller concentrations of other PTEs, without O), *Fe-silicates* (consisting mainly of Fe, Si and O), *Sulphates/Sulphides* (particles in which one of the main constituents is S), *Other metal oxides* (metal oxides excluding Fe), *Other metal alloys* (alloys of various metals, without Fe and O), *Spherical Si-particles* (spherical oxides consisting mainly of Si and/or other elements, such as Al, Ca, K, Mg) and *Other particles* (mainly minerals of geogenic origin, such as ilmenite and zircon). As the samples were placed on carbon tape and carbon-coated prior to the analysis in order to provide their conductivity, the presence of C in individual PTE-bearing particles could not be determined; therefore, some of the oxides might actually be carbonates.

## **2.5 Determination of oral bioaccessibility–Unified BARGE Method**

Oral bioaccessibility of selected PTEs was determined using the *in vitro* Unified BARGE Method (UBM). The UBM was firstly developed and validated for assessing bioaccessibility of As, Cd, and Pb in soil samples (Wragg et al., 2011; Denys et al., 2012) but during the following years its use was

expanded to the other elements (e.g. Barsby et al., 2012; Cruz et al., 2015; Qin et al., 2016) and media (e.g. Marinho-Reis et al., 2020; Zupančič et al., 2021). UBM simulate the physico-chemical conditions in the human mouth, stomach, and small intestine (e.g. pH, temperature, presence of enzymes, peristalsis, resident time) using the following synthetic analogue digestive fluids: saliva (pH =  $6.5 \pm 0.5$ ), gastric (pH =  $1.1 \pm 0.1$ ) and duodenal (pH =  $7.4 \pm 0.2$ ) fluids, and bile (pH =  $8.0 \pm 0.2$ ). Detailed compositions of digestive fluids are given in Wragg et al. (2009, 2011). Using UBM, oral bioaccessibility of As, Cd, Cr, Cu, Hg, Ni, Pb, Sb, Sn, and Zn was determined in the following 5 samples of attic dust (Fig. 1): MBAD02 (old town centre), MBAD07 (Studenci industrial zone), MBAD14 (Melje industrial zone), MBAD17 (newer residential area, close to the Tezno industrial zone), and MBAD21 (Tezno industrial zone). UBM was performed at the British Geological Survey. The following description of the method is partially summarised after Wragg et al. (2009, 2011). The UBM procedure runs in two parallel phases (gastric (G) and gastrointestinal (GI) phase) which results in two supernatants of each sample at the end of the procedure. A 0.6 g of dried and sieved (<0.063 mm) sample is used for each phase. The UBM method consists of three stages. In the first stage, sample is mixed with 9.0 mL of saliva and shaken for 10 seconds. Then 13.5 mL of gastric fluid is added and the pH is checked. If pH is not 1.2, adjustment with 1 M NaOH and/or 37% HCl is performed. This procedure is repeated until pH stabilizes at 1.2. The reaction tubes were then placed in an end-over-end rotator which is submerged in a water bath heated at 37 °C. After one hour of agitation, the pH is checked. The whole procedure should be repeated if the pH was higher than 1.7. The gastric phase samples are then centrifuged for 15 minutes at 4500 g. Supernatants of G phase were collected by pipetting and acidified with 500 µL of HNO<sub>3</sub> (67%). On the other hand, the gastrointestinal phase continues with adding 27 mL of duodenal fluid and 9 mL of bile fluid and adjusting the pH to 6.3 with NaOH or HCl. Tubes are then again placed into end-over-end rotator submerged in a water bath (37 °C). After four hours of agitation, the pH is noted and samples are centrifuged for 15 minutes at 4500 g. Supernatants of GI phase were collected and acidified with 1.0 mL of HNO<sub>3</sub> (67%). The levels of 10 PTEs in G and GI phases were measured with ICP-MS. Bioaccessible fractions (BAFs) of each PTE in both phases were calculated using equation [1].

$$BAF (\%) = \frac{\text{bioaccessible level of PTE } \left(\frac{\text{mg}}{\text{kg}}\right)}{\text{total level of PTE } \left(\frac{\text{mg}}{\text{kg}}\right)} \times 100 (\%)$$

[1]

The quality of the UBM analyses was ensured in several ways. The accuracy of the extraction protocol was estimated by analysing the BGS guidance material 102 (replicated 5 times), which provides guidance values for seven of the ten analysed PTEs (exceptions are Hg, Sb, Sn) in gastric phase (Hamilton et al., 2015). The accuracy, expressed as relative error (RE), was <5% for all PTEs, for which guidance values are available in the literature (Hamilton et al., 2015). The replicate of sample MBAD21 was added to sample batch to establish the precision of the analyses. The precision, expressed as relative percent difference (RPD), was between 0.1% (Ni) and 11.7% (Pb) in the gastric phase, and <20% for all PTE, except for Pb (RPD = 50%) and Zn (RPD = 36%), in the gastrointestinal phase. Additionally, a blank sample (containing only synthetic digestive fluids) was also analysed. The overall quality of UBM analyses was satisfactory for all elements, only the results of Pb and Zn in gastrointestinal phase should be interpreted with prudence.

## 2.6 Statistical treatment

Statistical treatment of the analytical data was performed using STATISTICA 13.5 software. The statistical distribution of the element levels was determined by a visual inspection of the histograms, by calculating skewness and kurtosis, and by applying the Shapiro-Wilk test. To identify potential grouping of the elements, a cluster analysis (Ward's method, 1-Pearson r) was performed. As the majority of the elements had a non-normal distribution, a box-cox transformation of the data set was done before cluster analysis to obtain close-to-normal distribution of the data. To define if the differences in chemical composition of attic dust between industrial and residential areas are statistically significant, the nonparametric Mann–Whitney U test was used.

Besides the study of attic dust as an individual media, its comparison with soil chemistry can provide valuable additional indices on past anthropogenic emissions. A direct comparison of chemical composition is not appropriate owing to their different formation/origin, physico-chemical and biological processes and resident times, as well as their different levels of exposure to weather conditions. Calculation of normalised enrichment factors (EF) is a suitable tool for such comparison since normalisation to some extent reduces these differences between the attic dust and soil. The normalised EF can be used to distinguish between the chemical elements of prevailing natural and anthropogenic origin and to assess the degree of human influence on their distribution (Yongming et al., 2006). This approach is appropriate for our case study since majority of the elements are under the influence of geogenic factors in the soil of Maribor (with the exception of Cu, Pb, and Zn) (Gaberšek & Gosar, 2018). The normalised EF of all elements were calculated (with the exception of Te and W for which soil data are not available) using equation [2], where  $Md_x$  (AD) is a median level of selected element in attic dust,  $Md_{Al}$  (AD) a median level of aluminium in attic dust,  $Md_x$  (SO) a median level of selected element in soil, and  $Md_{Al}$  (SO) a median level of aluminium in soil. The soil data were taken from Gaberšek & Gosar (2018; 118 sampling sites in a  $500 \times 500$  m grid, upper 10 cm of soil, pulverised fraction of  $<2$  mm, aqua regia digestion, ICP-MS). Aluminium was used for normalisation, as its levels and spatial distributions in both media from Maribor are subject to natural/geogenic factors.

$$EF = \frac{\frac{Md_x(AD)}{Md_{Al}(AD)}}{\frac{Md_x(SO)}{Md_{Al}(SO)}}$$

[2]

The  $EF < 2$  indicates Deficiency to minimal enrichment,  $2 < EF < 5$  Moderate enrichment,  $5 < EF < 20$  Significant enrichment,  $20 < EF < 40$  Very high enrichment, and  $EF > 40$  Extremely high enrichment (Barbieri, 2016).

The point symbol geochemical maps for 47 PTEs (for REE only maps of Ce, Dy, La, and Yb were made) in attic dust were produced in order to present their spatial distribution. Point maps of Cu, Mo, Pb, and Zn were additionally plotted on interpolated soil geochemical maps that were produced based on the soil survey presented by Gaberšek & Gosar (2018) and by using Natural neighbour interpolation method. Seven percentile classes were chosen for plotting point symbol maps of element levels in attic dust (0–10, 10–25, 25–40, 40–60, 60–75, 75–90, and 90–100%). The same percentile classes were used for interpolated soil geochemical maps, only the last one was divided into two classes (90–95, 95–100%) to further emphasise the areas with the exceptionally high levels of PTEs. Geochemical maps were produced with QGIS.

### **3. Results and Discussion**

#### **3.1 Element levels in attic dust and their spatial distribution**

The descriptive statistics of the chemical analysis of attic dust is given in Table 1. The raw data for each sampling site is presented in Appendix SM2 and point geochemical maps of 47 elements in Appendix SM3 (Figures SM3.1-SM3.47) in the supplementary material. The levels of chemical elements vary considerably between sampling sites, in particular levels of PTEs. With the use of cluster analysis, we identified two groups of PTEs of predominantly anthropogenic origin, presumably industrial. The first one consists of two subgroups: Co-Fe-Mo-Ni-W and Ba-Cr-Mg-Mn-Nb-Ti (Fig. 2). Levels of Co, Cr, Fe, Mo, Nb, Ni, W, and also Bi are statistically significantly ( $p < 0.05$ ) higher in the industrial zone Tezno (sampling sites MBAD20-close to industrial zone, and MBAD21-within industrial zone) than in other town's areas. The highest levels of Ba, Mg, and Mn were also detected at MBAD21 but the differences to other sampling sites are not statistically significant. The levels of Cr, Mo, and, W are particularly higher in Tezno (their levels at sampling site MBAD21 are 184 mg/kg, 36 mg/kg, 41 mg/kg, respectively) (Appendix SM2) than the median levels of the whole sample batch (61 mg/kg, 5.5 mg/kg, 2.6 mg/kg, respectively). Example of Mo spatial distribution in attic dust and soil is given in Fig. 3 and spatial distribution of other elements in Appendix SM3. The Tezno industrial zone was dominated by a large truck and bus factory (TAM) in the past, together with some other metal processing factories (e.g. crane plant). Today, there are

several smaller automotive and metal processing factories and waste treatment plants. Many of the PTEs in this group have been associated with emissions from the ironworks and steel industry in the past (Šajin, 2003; Teran et al., 2020). We assume that the highest levels of these PTEs are mainly due to metal-processing industry in this area. On the other hand, Co, Cr, Fe, Mn, and Ni can be partially associated also with the weathering of the igneous and metamorphic rocks in the wider Maribor area.

The other group of anthropogenic-derived PTEs consists of Be-Cd-Cu-Sb-Sn-Pb-Te-Zn (Fig. 2). Their highest levels are typical for the Melje industrial zone (MBAD13, MBAD14) and surroundings areas (MBAD06) (Fig. 3, Appendix SM2, Appendix SM3) and are statistically significantly ( $p < 0.05$ ) higher than in other sampling sites through the town. This relatively small area has a century-long tradition of various industrial activities. Among others, the area was home to a battery factory (now closed), foundry (manufacturing products from Cu-alloys (e.g. brass, bronze) and various steel tools) and a metal furniture factory. The determined levels of Cu (2115, 1908 and 726 mg/kg), Pb (1208, 985 and 654 mg/kg), Sn (74, 55 and 52 mg/kg), and Zn (6269, 5735 and 5528 mg/kg) in attic dust in the three samples from Melje (MBAD06, MBAD13, MBAD14) are considerably higher than their median levels for the whole sample batch (193 mg/kg, 424 mg/kg, 23 mg/kg, and 1478 mg/kg, respectively). Based on data of past industrial activities in the Melje industrial zone, the battery factory was probably an important source of Pb, and foundry a source of Cu, Sn, and Zn. Other PTEs could have been used as alloy additives whether they were contained in the input raw material as impurities and omitted in the surroundings during the industrial processes. The spatial distribution of Cu, Pb and Zn levels in attic dust, with their highest levels in the Melje industrial zone, only partially corresponds with their soil distribution (Fig. 3). The areas with the highest levels in soil are much more unevenly distributed through the town. These differences may be the result of a denser and more evenly distributed soil sampling sites (Gaberšek & Gosar, 2018), localised PTEs sources, and the use of allochthonous contaminated soil throughout the town.

In addition to the industrial sources of PTEs, some other past (and present) anthropogenic sources are suggested. Coal combustion is a known source of SO<sub>2</sub>, Se, Hg, Tl, As (Pacyna & Pacyna, 2001) as well as Ag, U, and other PTEs (Nalbandian, 2012). The results of the cluster analysis (Fig. 2) indicate a common source for these elements in the Maribor area. Their highest levels are often detected in the wider area of the old town centre. Calcium and Sr might originate from construction activities, degradation of building materials, and winter road maintenance. The spatial distribution (Appendix SM3) and levels of some of the remaining elements (Al-Cs-Ga-Hf-Li-Na-Rb-Sc-Th-Y-V-Zr-REE) predominantly reflect the natural/geogenic conditions in the area, particularly the weathering of igneous and metamorphic rocks. Their levels are evenly dispersed through the town without any clear spatial distribution patterns. Phosphorus can be associated with the presence of pigeon excrement in the attics.

Normalised EF were calculated to get an additional insight into the geochemical properties of attic dust and to assess the degree of human influence on levels and distribution of elements. In comparison to soil, attic dust shows extremely high enrichment with S (EF=147) and very high enrichment with Zr (EF=25). Significantly enriched ( $5 < EF < 20$ ) are the following 14 elements: Na, Zn, Sb, Sn, Pb, Cd, Ag, Mo, Bi, Sr, B, Ca, Cu, and, Se. An additional 13 elements have  $EF > 2$  (Table 1). Most of the enrichments probably originate from the above described anthropogenic sources (industrial activities and coal combustion). The EF calculation revealed several other significantly enriched elements of potentially anthropogenic origin which were not identified by the cluster analysis. These are Zr, Na, and B. While the reasons for Zr and B (its highest level of 290 mg/kg was identified in the residential area, near the park forest) enrichments in Maribor is not yet identified, Na may originate from winter road salting and also from geogenic sources (e.g. Na-feldspar). The EF calculation separately for the Melje industrial zone and Tezno industrial zone showed similar results. In Melje, S shows extremely high enrichment and Zn, Pb, Cd, Sb, Na, Cu, Sn, Zr, Ag, Mo, Se, and Bi significant enrichment. In the Tezno zone, S again shows extremely high enrichment and the following elements significant enrichment: Bi, Na, B, Zr, Cr, Sr, Cd, Ag, Ca, Zn, Pb, Nb, Sb, and Ni. The determined enrichments in attic dust in Maribor as a whole and in two industrial zones indicate that attic dust responds much

faster to the airborne anthropogenic contamination than soil. The reason for that are the differences in physico-chemical and biological processes occurring in them and their different resident times. The anthropogenically-derived PTE-bearing particles deposit in attics and remain there undisturbed for a longer period of time. On the other hand, in soil they are exposed to weather conditions, erosion and transportation as well as mixing with soil matrix (e.g. organic matter and clay minerals) which somehow dilute the amount of contaminants in soil.

### 3.2 Mineral and phase composition of attic dust

In previous study (Gaberšek & Gosar, 2021b), the presence of gypsum and silicates, of which quartz predominates over plagioclase, muscovite/illite, and chlorite, was determined in two attic dust samples with X-ray powder diffraction (XRD). The presented study supplemented XRD analysis by surface EDS analysis (mapping), which was performed on four samples. This method enables assessment of not only mineral phases but also other phases, like carbon-rich and PTE-bearing particles, and also phases with small abundances. On average, attic dust mainly consists of **gypsum/anhydrite** (45%) and **silicates** (33%), followed by **carbon-rich particles** (8.3%), **carbonates** (8.1%), and **PTE-bearing particles** (5.3%) (Table 2). Silicate minerals originate from local geogenic sources (weathering and erosion of igneous and metamorphic rocks and sediments as well as soil), while carbonates, carbon-rich and PTE-bearing particles originate predominantly from anthropogenic sources. Nevertheless, natural/geogenic sources cannot be completely excluded. Gypsum (Fig. 4a) is probably of secondary origin. Secondary sulphate minerals, especially gypsum ( $\text{CaSO}_4 \cdot 2\text{H}_2\text{O}$ ), glauberite ( $\text{Na}_2\text{Ca}(\text{SO}_4)_2$ ) and thenardite ( $\text{Na}_2\text{SO}_4$ ) have also been discovered in some previous studies of attic dust (Šajn, 1999; Baricza et al., 2016; Miler & Gosar, 2019). They are most likely formed *in situ* in attics by a reaction of  $\text{SO}_2$  gas from the atmosphere (originating mainly from anthropogenic sources, especially combustion processes in power plants, industry, and traffic) and Ca- as well as Na-bearing particles in the dust (e.g. calcite, plagioclase) (Baricza et al., 2016). Similar processes also occur on the carbonate facades of buildings and monuments in areas characterised by  $\text{SO}_2$  contamination (Frank-Kamenetskaya et al., 2009; Baricza et al., 2016). The crystallisation of gypsum is a relatively rapid process. Ausset et al. (1999) determined the presence of gypsum crystals

on the surface of fly-ash particles after three months of their exposure to  $\text{SO}_2$  ( $340 \mu\text{g}/\text{m}^3$ ) and high relative humidity (79%). Emissions of  $\text{SO}_2$  were much higher in the past than they are today. In Slovenia, they fell by 94% over the period 1980–2007 (Rode, 2009). The Ca-bearing particles in Maribor can originate from outside sources (e.g. winter road gritting with carbonate sand) and degradation of carbonate building material within the attics (e.g. lime plaster, concrete). Some studies indicate that gypsum can also originate from external anthropogenic sources, like coal combustion (Jabłońska & Janeczek, 2019) and sulphide ore smelting (Miler & Gosar, 2019).

The proportions of determined phases vary slightly between individual samples (Table 2). The sample from the Tezno industrial zone (MBAD21) differs most from the others. There we find the highest proportions of PTE-bearing particles (12%) and dolomite (13%) and the lowest proportion of gypsum (30%). These proportions are in agreement with the results of the chemical analysis, which showed the highest level of Mg (2.59 %) and the lowest level of S (1.93%) in the sample from Tezno. One possible explanation for the lowest level of S and the lowest proportion of gypsum on the one hand and the highest proportion of carbonates on the other might lay in the fact that this building is the youngest of all the sampling sites, thus the short reaction time for the carbonate particles and  $\text{SO}_2$ , which may have resulted in a smaller quantity of gypsum being crystallised.

### 3.3 Characteristics and origin of PTE-bearing particles

The size, morphological characteristics, and chemical composition of a total of 1294 PTE-bearing particles in four samples were analysed. Their mean size was  $4.3 \mu\text{m}$ . In total, most of the PTE-bearing particles were listed in a group of Fe-oxides (618 particles, 48%), followed by a group of Sulphates/Sulphides (211 particles, 16%) and Spherical Fe-oxides (156 particles, 12%). On the other hand, only a few Fe-silicate particles (0.2%) and Other metal alloys (0.5%) were identified (Table 3). Proportions of the determined groups of PTE-bearing particles vary considerably between the different areas of the town (Table 3). Nevertheless, **Fe-oxide** particles predominate in all samples of attic dust (from 40% in the old town centre to 54% in the Tezno industrial zone). Along with Fe and O, they often contain minor amounts of other PTEs (e.g., Mn, Cu, Cr, Zn) and are largely angular and

irregular in shape. The characteristics of the Fe-oxides from the Tezno industrial zone differ slightly from other sites. Thin sharp-edged shavings (Fig. 4b), partially melted particles, irregularly shaped particles with a smooth, glassy, or porous surface and various fragments are more common at Tezno than elsewhere. Nickel- and W-rich particles (Fe-W-Cu-O and Fe-W-Co-O (Cr)) were also identified. The particles of above presented morphological characteristics and chemical composition do not originate from natural sources, but from anthropogenic processes. Their source in the Tezno industrial zone is probably metal-processing industry. On the other hand, angular Fe-oxides can originate from both geogenic and anthropogenic sources (Slezakova et al., 2008; Miler, 2020).

While distinguishing between natural and anthropogenically-derived angular particles of Fe-oxides might be a challenging task, several PTE-bearing particle types are certainly of anthropogenic origin: Spherical Fe-oxides, Fe-alloys, Other metal alloys, and Spherical Si-particles. On average, these four groups combined represent 25% of all PTE-bearing particles. The highest proportion of **Spherical Fe-oxides** was identified in the Tezno industrial zone (19%) and the lowest in the Melje industrial zone (4.6%). They can be full or hollow (Fig. 4c), with smooth, porous, skeletal-dendritic (Fig. 4d) or plated surfaces, often containing minor amounts of Cu, Mn, and Zn. Mn-containing spheres are more common in the sample from Tezno industrial zone than in other samples. The highest proportions of Fe-oxide and Spherical Fe-oxide particles in the sample from Tezno industrial zone correspond well with the determined highest levels of Fe and some other PTEs in the same sample. In contrast to Spherical Fe-oxides, the proportion of **Spherical Si-particles** is higher in residential areas than in industrial areas. They contain a plethora of elements (e.g., Al, Ca, Fe, K, Mg, Ti, Cr, Cu, Mn, Zn) in varying amounts. Spherical Fe-oxides and Si-particles originate from high temperature anthropogenic processes, like the steel industry, metallurgical processes, and the combustion of fossil fuels (Sokol et al., 2002; Umbria et al., 2004; Ebert et al., 2012; Miler and Gosar, 2015; Talovskaya et al., 2017). The highest proportion of **Fe-alloys** was identified in both industrial zones. In the Tezno industrial zone we identified mainly particles of pure Fe alloys and Fe alloys with minor amounts of Cu, Cr, and Mn. The composition of these types of particles in the Melje industrial zone were slightly more complex. We found individual particles of Fe-Ni-V, Fe-Cr-Si (Cu, Zn), Fe-Zn (Mn), Fe-Cr (Cu, Ni, Ca) and

others. Most of the Fe-alloy particles occur in the form of shavings, irregularly shaped particles, and also as spherules. Particles of the group of **Other metal alloys** were identified only in the Melje industrial zone, consisting only of Cu-Zn particles with minor amounts of Pb, Cl, and Fe (Fig. 4e). They occur mainly as relatively large shavings with a mean size of 20.8  $\mu\text{m}$ . Some of them have Cu-S-Cl crystals on their surface (Fig. 4f), which are probably the result of an *in-situ* reaction between the deposited particles and atmospheric  $\text{SO}_2$ . This assumption is confirmed by a comparison of the same particle type from this area in other media (street dust, snow, airborne PM), where such crystals do not occur (Gaberšek & Gosar, 2021b). Cu-Zn (Pb, Cl, Fe) particles originate from a nearby foundry that has been manufacturing products from Cu-alloys and various steel tools for almost a century. The occurrence of this particle type coincides with the highest total levels of Cu and Zn in attic dust.

The group of **Sulphates/Sulphides** is represented mainly by Ba-S-O particles (possible mineral: barite) which often contain some Zn. They might originate from natural or anthropogenic sources. One of the possible anthropogenic sources is the degradation of white wall paint, where barite and lithopone (a mixture of barium sulphate and zinc sulphide) are used as white pigments (van Alphen, 1998). Pb-sulphates are also common in some samples. Pb-S-O (Cu, Zn) particles (Fig. 4g) were found at sampling sites MBAD09 (close to Tezno) and MBAD14 (Melje) where they represent 2.5% and 6.1% of all PTE-bearing particles, respectively. They can originate from geogenic sources (possible mineral: anglesite) or from industrial processes at the former battery factory in Melje and/or from metal industry in Tezno. Another type of Pb-sulphates identified is K-Pb-S-O (Cu, Zn) (possible mineral: palmierite; Fig. 4h), which was discovered in all samples, with the exception of a sample from the old town centre. The highest proportions were found in samples from and close to the Tezno industrial zone (MBAD21 and MBAD09, respectively). As geogenic palmierite is found in volcanic fumaroles, its anthropogenic origin in the area of Maribor is more likely. K-Pb sulphates commonly occur in Pb- reverberatory smelting slags (Lead Reach Consortium, 2012) and in secondary Pb-smelter fly ash that has been exposed to acidic conditions (pH 3–5) (Vítková et al., 2009). Miler & Gosar (2019) associated Pb-S-O (Cu, Zn) particles present in attic dust with primary Pb- smelting and K-Pb-S-O particles with secondary Pb- recycling.

The group of **Other metal oxides** consists mainly of Cu, Pb and Zn oxides/carbonates, with the highest proportion found in the Melje industrial zone. Their origin is not precisely defined, as they can originate from both geogenic and anthropogenic sources. Two potential historic anthropogenic sources in Melje are battery factory and foundry. Particles of the groups of **Fe-silicates** and **Other particles** largely originate from geogenic sources. The proportions of the group of Other particles are highest at two non-industrial sampling sites (Table 3). It is mainly represented by the following minerals originating from the weathering of igneous and metamorphic rocks: Ti-O (mineral rutile), Fe-Ti-O (often with Mn; mineral ilmenite), Zr-Si-O (mineral zircon) and Ce-La-P-O (mineral monazite).

### 3.4 Oral bioaccessibility of PTEs

Oral bioaccessibility differs strongly between individual PTEs, samples, and both phases—gastric (G) and gastrointestinal (GI) (Fig. 5, Appendix SM1-Table S2). Mean bioaccessible fractions (BAFs) in gastric phase are decreasing as Cd>Zn>Pb>Cu>As>Ni>Cr>Sb>Hg>Sn, and in gastrointestinal phase as Cu>Cd>Ni>As>Sb>Zn>Hg>Cr>Pb>Sn. The BAFs of most elements are higher in the gastric than in the gastrointestinal phase. The only exceptions are Cu, Hg, and Sb with a slightly higher mean BAF in the GI phase (40%, 7.6%, and 17%, respectively) than in G phase (37%, 6.9%, and 15%, respectively). The highest BAFs in the gastric phase have Cd (range of 59–70%; mean of 66%), Zn (range of 58–75%; mean of 65%), and Pb (range of 5.6–65%; mean of 43%). The lowest mean BAFs in the gastric phase were determined for Sn (2.5%) and Hg (6.9%), while mean gastric BAFs of As, Cr, and Ni are 34%, 17%, and 29%, respectively. The bioaccessibility of most elements drops significantly after the transition from the stomach to the small intestine. The mean BAFs of Cd, Cr, Pb and Zn fall to 32%, 3.8%, 2.1% and 13%, respectively. The mean BAF of Ni only falls by 3%. By far the lowest BAF in GI phase has Sn (0.4%). The reason for the general decrease in BAFs in the GI phase is an increase in pH value in the small intestine. Low pH is typical for the stomach environment and close to neutral values are typical for the small intestine (Ruby et al., 1996). Changes in pH may result in the precipitation of PTE phases that were previously dissolved in the stomach. In general, the

most unstable mineral phases in the acidic stomach environment are oxides, some sulphides, and carbonates (Grøn & Andersen, 2003). The presence of Cu, Pb, and Zn oxides/carbonates and sulphides in attic dust was confirmed with SEM/EDS analysis, while Cd-particles were not identified. On the other hand, the increase of BAFs of Cu, Hg, and Sb in 4 out of 5 samples (interestingly, the only exception for all three PTEs is sample MBAD17) and Ni in the sample MBAD21 in the GI phase might be the result of the formation of complexes (e.g. with enzyme pepsin) or the dissolution of PTE-bearing organic matter, which can occur at neutral pH in the small intestine (Grøn & Andersen, 2003).

One of the well-known characteristics of bioaccessibility is that the highest total PTEs levels do not necessarily result in the highest bioaccessibility, regardless the general high correlations observed between the two (Barsby et al., 2012; Qin et al., 2016). In our study, this is most obvious in the case of a sample from the Tezno industrial zone (MBAD21). It has the highest total levels of Cr (184 mg/kg) and Ni (104 mg/kg), of which only 11.8 mg/kg (6.4%) of Cr and 17.5 mg/kg (17%) of Ni are bioaccessible in the gastric phase, and 2.1 mg/kg (1.2%) and 20.2 mg/kg (19%) in the gastrointestinal phase (Fig. 5). Additionally, the BAF of Cu and Pb in the same sample are also distinctly lower than in other samples. It seems that many of the analysed PTEs occur in much more stable chemical compounds in the Tezno industrial zone than elsewhere in the town.

The direct comparison of presented results with the only known past study of PTEs bioaccessibility in attic dust (Bačeva-Andonovska et al., 2015) is not possible due to different methods used. On the other hand, there are numerous studies of bioaccessibility in soil (e.g. Barsby et al., 2012; Qin et al., 2016; Fernandez-Landero et al., 2021) and in household dust (Marinho-Reis et al., 2020; Zupančič et al., 2021) that also used UBM. Although results of these studies somewhat differ, there are some general trends observed regardless of the media studied, and also similarities with the presented study: most PTEs have higher BAFs in gastric than in gastrointestinal phase; PTEs with the highest BAFs in gastric phase are usually Cd, Cu, Pb, and Zn, while the most bioaccessible PTEs in gastrointestinal phase are various; relatively high correlation between total levels and their bioaccessible levels are

normally determined. Comparison of BAFs between the media indicate that BAFs in household dust may be higher than in soil. For example, mean BAFs of Cd, Cu, Pb, and Zn in gastric phase in soil of Northern Ireland (Barsby et al., 2012) are 49%, 31%, 33%, and 22%, respectively, while in household dust from the town of Idrija, Slovenia (Zupančič et al., 2021) are 80%, 35%, 82%, and 77%. Similarly high gastric BAFs of Cd (81%), Pb (60%), Zn (84%) in household dust were determined also by Marinho-Reis et al. (2020).

### **3.5 Is attic dust a hazardous material?**

Although attic dust may contain high levels of PTEs, it is usually not addressed as a hazardous material in the scientific literature. This is because it accumulates and remains undisturbed in attics for decades. As such, it is used as a proxy for historical air contamination rather than treated as hazard to human health. Nevertheless, Davis & Gulson (2005) emphasised that attic dust may act as a source of recent contamination in cases of the renovation and demolition of old buildings, and in case of migration of dust particles through openings into inhabited parts of buildings. The United States Environmental Protection Agency has also stated that attic dust should be taken into consideration if high Pb levels in blood of children living on the site cannot be explained by other sources (USEPA, 2008). The presented study of oral bioaccessibility of PTEs in attic dust, which is to the best of our knowledge, only the second study of this kind, showed high BAFs of As, Cd, Cu, Pb, and Zn in gastric phase, and high BAFs of As, Cd, Cu, and Ni in gastrointestinal phase. This indicate that some negative health effects may occur in the case of ingestion of attic dust. Since the absorption of nutrients and PTEs is much higher in small intestine than in stomach (Kiela & Ghishan, 2016), the high stomach BAFs do not necessarily present bigger hazard to health than lower gastrointestinal BAFs. On the other hand, low bioaccessible fraction do not necessarily mean low hazard to health in cases of high total PTEs levels and long-term exposure. The positive aspect is that we are usually not frequently in the prolonged contact with attic dust. Some potential exposure pathways to attic dust for inhabitants are frequent activities in the attics (children playing, cleaning, etc.), placing or retrieving storage items, migration of dust through openings and cracks in walls and ceiling into inhabited parts of buildings which can be problematic especially in old buildings and if part of the attic is converted

into living space. As already mentioned by Davis & Gulson (2005) demolition of old buildings and renovations may temporarily increase the dust load in the living spaces of the home on the one hand and represent a hazard to health to the construction workers who are frequently in contact with these conditions on the other hand. The potential for exposure to contaminants in attic dust may be reduced if the attic is well-sealed from the living space (USEPA, 2008). The presented result and data from past studies indicate that attic dust should be considered as a hazardous material for human health, especially in the areas of known long-term pollution processes, like historical mining sites, and in old residential buildings. Additional studies of human exposure to attic dust and its potential hazard to human health warrants further study, in particular simulations of lung inhalation or dermal absorption of PTEs contained in attic dust as a pathway of exposure to better inform possible hazards to human health.

#### **4. Conclusions**

Due to its accumulative nature, attic dust is normally addressed as an excellent proxy for historical air contamination, which was shown by this study and the wider literature. The detailed determination of its bulk chemical composition and morphological as well as chemical characterisation of individual solid particles enables identification of dust sources and also processes that occur within attics. In the case of Maribor, we identified pronounced influence of past industrial activity in Melje and Tezno industrial zones as well as coal burning reflected by high levels of some PTEs and occurrence of specific PTE-bearing particles. The Melje industrial zone is characterised by the highest levels of Be, Cd, Cu, Pb, Sb, Sn, Te, and Zn, as well as the occurrence of Cu-Zn shavings and a high proportion of Pb-sulphates. On the other hand, the highest levels of Co, Fe, Mo, Ni, W, Ba, Cr, Mg, Mn, Nb, and Ti, as well as the highest proportion of PTE-bearing particles, in particular groups of Fe-oxides and Spherical Fe-oxides, were identified in the Tezno industrial zone. These characteristics reflect the different past industrial activities of the two areas: the foundry and battery factory in Melje, and the metal-processing and automotive industry in Tezno. The prevailing mineral in attic dust is gypsum, which was presumably formed in situ by the reaction of  $\text{SO}_2$  gas from the atmosphere with carbonate dust particles. One of the main sources of  $\text{SO}_2$  emissions as well as emissions of Se, Hg, Tl, As, Ag,

and U was coal combustion. The crystallisation of gypsum and some other in situ changes on deposited particles (e.g. formation of Cu-S-Cl crystals on Cu-Zn particles) indicates that attic dust is not a stable and isolated media, and that some physico-chemical changes occur over time. Natural/geogenic effects on the attic dust are characterised by the presence of minerals originating mainly from the weathering of igneous and metamorphic rocks (e.g. rutile, ilmenite, zircon, monazite, quartz, and other silicates).

The presented research provided new information to inform the potential hazard to human health associated with attic dust by determining the oral bioaccessibility of 10 PTEs. Although attic dust is usually not considered as a hazardous material, high levels of some PTEs, high mean BAFs of As, Cd, Cu, Pb, and Zn in the gastric phase and the high BAFs of As, Cd, Cu, and Ni in the gastrointestinal phase, as well as the potential for long-term exposure, discussed here, indicate that attic dust may pose a hazard to human health if it is disturbed.

The presented research is one of the first known steps towards identification of hazard to human health of attic dust. In the future, the study of oral bioaccessibility should be complemented with simulations of lung inhalation or dermal absorption of PTEs contained in attic dust as a pathway of exposure to better inform possible hazard to human health. Consideration of attic dust as a proxy for historical air contamination and/or as a hazard to human health may have several implications for inhabitants of industrial and post-industrial urban areas. A detailed study, addressing the whole life cycle of the attic dust, similarly as was presented here, should be done in such locations. Special attention should be paid to the potential exposure of inhabitants in older buildings and close to past emission sources. In heavily polluted areas some measures might be needed, like sealing of attics to avoid migration of dust to living spaces or even removal of hazardous dust.

## Acknowledgements

The presented study was funded by the Slovenian Research Agency (ARRS) in the frames of the research programme “Groundwater and Geochemistry” (P1-0020), the research project “Dynamics and matter flow of potentially toxic elements (PTEs) in urban environment” (J1-1713), and infrastructure programme “Geological information centre” (I0-0007 (A)). Financial assistance was also provided by the “Slovenian National Commission for UNESCO, National Committee of the International Geosciences and Geoparks Programme”. We thank Prof. Dr. Nina Zupančič and Dr. Miloš Miler for their helpful comments and suggestions.

## CRedit authorship contribution statement

**Martin Gaberšek:** conceptualization, data curation, methodology, formal analysis, investigation, resources, writing - original draft, visualization. **Michael J. Watts:** methodology, writing - review & editing. **Mateja Gosar:** conceptualization, methodology, writing - review & editing, supervision.

## 5. References

Ali, M.U., Liu, G., Yousaf, B., Ullah, H., Abbas, Q., Munir, M.A.M., 2019. A systematic review on global pollution status of particulate matter-associated potential toxic elements and health perspectives in urban environment. *Environ. Geochem. Health* 41, 1131–1162. <https://doi.org/10.1007/s10653-018-0203-z>

Ausset, P., Del Monte, M., Lefèvre, R.A., 1999. Embryonic sulphated black crusts on carbonate rocks in atmospheric simulation chamber and in the field: role of carbonaceous fly ash. *Atmos. Environ.* 33, 1525–1534. [https://doi.org/10.1016/S1352-2310\(98\)00399-9](https://doi.org/10.1016/S1352-2310(98)00399-9)

Bačeva Andonovska, K., Stafilov, T., Karadjova, I., 2015. Assessment of trace elements bioavailability – ingestion of toxic elements from the attic dust collected from the vicinity of the ferro-nickel smelter plant. *Contributions, Sec. Nat. Math. Biotech. Sci., MASA* 36, 93–104. <http://dx.doi.org/10.20903/csnmbs.masa.2015.36.2.71>

Balabanova, B., Stafilov, T., Šajn, R., Tănăselia, C., 2017. Long-term Geochemical Evolution of Lithogenic Versus Anthropogenic Distribution of Macro and Trace Elements in Household Attic Dust. *Arch. Environ. Contam. Toxicol.* 72, 88–107. <https://doi.org/10.1007/s00244-016-0336-y>

Barbieri, M., 2016. The Importance of Enrichment Factor (EF) and Geoaccumulation Index (Igeo) to Evaluate the Soil Contamination. *J. Geol. Geophys.* 5, 4 pp. <https://doi.org/10.4172/2381-8719.1000237>

Baricza, Á., Bajnóczi, B., Tóth, M., Káldos, R., Szabó, C.S., 2016. Characterization of particulate matter in attic and settled dusts collected from two buildings in Budapest, Hungary. In: Prikryl, R., Török, A., Gomez-Heras, M., Miskovsky, K., Theodoridou, M. (eds.). 2016. Sustainable Use of Traditional Geomaterials in Construction Practice. Geological Society of London, Special Publication 416, 239–252. <https://doi.org/10.1144/SP416.14>

Barsby, A., McKinley, J.M., Ofterdinger, U., Young, M., Cave, M.R., Wragg, J., 2012. Bioaccessibility of trace elements in soils in Northern Ireland. *Sci. Total Environ.* 433, 398–417. <https://doi.org/10.1016/j.scitotenv.2012.05.099>

Bertalanič, R., 2007. Wind levels in Slovenia in 2006. *Ujma* 21, 27–36. <http://www.sos112.si/slo/tdocs/ujma/2007/027.pdf>

Calvo, A.I., Alves, C., Castro, A., Pont, V., Vicente, A.M., Fraile, R., 2013. Research on aerosol sources and chemical composition: Past, current and emerging issues. *Atmos. Res.* 120–121, 1–28. <https://doi.org/10.1016/j.atmosres.2012.09.021>

Cizdziel, J.V., Hodge, F.V., Faller, S.H., 1998. Plutonium anomalies in attic dust and soils at locations surrounding the Nevada test site. *Chemosphere* 37, 1157–1168. [https://doi.org/10.1016/S0045-6535\(98\)00107-6](https://doi.org/10.1016/S0045-6535(98)00107-6)

Cizdziel, J.V., Hodge, V.F., 2000. Attics as archives for house infiltrating pollutants: trace elements and pesticides in attic dust and soil from southern Nevada and Utah. *Microchem. J.* 64, 85–92. [https://doi.org/10.1016/S0026-265X\(99\)00018-1](https://doi.org/10.1016/S0026-265X(99)00018-1)

Coronas, M.V., Bavaresco, J., Vaz Rocha, J.A., Geller, A.M., Caramão, E.B., Rodrigues Kolowski, M.L., Vargas Ferrão, V.M., 2013. Attic dust assessment near a wood treatment plant: past air pollution and potential exposure. *Ecotoxicol. Environ. Saf.* 95, 153–160. <https://doi.org/10.1016/j.ecoenv.2013.05.033>

Cruz, N., Rodrigues, S.M., Tavares, D., Monteiro, J.R.J., Carvalho, L., Trindade, T., Duarte, A.C., Pereira, E., Römken, P.F.A.M., 2015. Testing single extraction methods and in vitro tests to assess the geochemical reactivity and human bioaccessibility of silver in urban soils amended with silver nanoparticles. *Chemosphere* 135, 304–311. <http://dx.doi.org/10.1016/j.chemosphere.2015.04.071>

Davis, J.J., Gulson, B.L., 2005. Ceiling (attic) dust: A “museum” of contamination and potential hazard. *Environ. Res.* 99, 177–194. <https://doi.org/10.1016/j.envres.2004.10.011>

Denys, S., Caboche, J., Tack, K., Rychen, G., Wragg, J., Cave, M., Jondreville, C., Feidt, C., 2012. In Vivo Validation of the Unified BARGE Method to Assess the Bioaccessibility of Arsenic, Antimony, Cadmium, and Lead in Soils. *Environ. Sci. Technol.* 46, 6252–6260. <https://doi.org/10.1021/es3006942>

Ebert, M., Müller-Ebert, D., Benker, N., Weinbruch, S., 2012. Source apportionment of aerosol particles near a steel plant by electron microscopy. *J. Environ. Monit.* 14, 3257–3266. <https://doi.org/10.1039/C2EM30696D>

Frank-Kamenetskaya, O.V., Vlasov, D.Y., Zelenskaya, M.S., Knauf, I.V., Timasheva, M.A., 2009. Decaying of the marble and limestone monuments in the urban environment. Case studies from Saint Petersburg, Russia. *Studia UBB Geologia*, 54, 17–22. <http://dx.doi.org/10.5038/1937-8602.54.2.4>

Fernández-Landero, S., Giráldez, I., Fernández-Caliani, J.C., 2021. Predicting the relative oral bioavailability of naturally occurring As, Cd and Pb from in vitro bioaccessibility measurement: implications for human soil ingestion exposure assessment. *Environ. Geochem. Health* 43, 4251–4264. <https://doi.org/10.1007/s10653-021-00911-4>

Gaberšek, M., Gosar, M., 2018. Geochemistry of urban soil in the industrial town of Maribor, Slovenia. *J. Geochem. Explor.* 187, 141–154. <https://doi.org/10.1016/j.gexplo.2017.06.001>

Gaberšek, M., Gosar, M., 2021a. Meltwater chemistry and characteristics of particulate matter deposited in snow as indicators of anthropogenic influences in an urban environment. *Environ. Geochem. Health.* 43, 2583–2595. <https://doi.org/10.1007/s10653-020-00609-z>

Gaberšek, M., Gosar, M., 2021b. Towards a holistic approach to the geochemistry of solid inorganic particles in the urban environment. *Sci. Total Environ.* 763, 13 pp. <https://doi.org/10.1016/j.scitotenv.2020.144214>

Gosar, M., Šajn, R., 2001. Mercury in soil and attic dust as a reflection of Idrija mining and mineralization (Slovenia). *Geologija* 44, 137–159. <https://doi.org/10.5474/geologija.2001.010>

Gosar, M., Šajin, R., Biester, H., 2006. Binding of mercury in soils and attic dust in the Idrija mercury mine area (Slovenia). *Sci. Total Environ.* 369, 150–162. <https://doi.org/10.1016/j.scitotenv.2006.05.006>

Grøn, C., Andersen, L., 2003. Human Bioaccessibility of Heavy Metals and PAH from soil. Environmental Project No. 840, Technology Programme for Soil and Groundwater Contamination. Danish Environmental Protection Agency, 16–21. [https://www.miljoeogressourcer.dk/filer/lix/2534/87-7972-878-2\\_\\_Environmental\\_Project\\_no.\\_840\\_\\_2003\\_.pdf](https://www.miljoeogressourcer.dk/filer/lix/2534/87-7972-878-2__Environmental_Project_no._840__2003_.pdf) Accessed April 6, 2021

Hamilton, M.E., Barlow, T.S., Gowing, C.J.B., Watts, M.J., 2015. Bioaccessibility performance data for fifty-seven elements in guidance material BGS 102. *Microchem. J.* 123, 131–138. <https://doi.org/10.1016/j.microc.2015.06.001>

Herath, I., Vithanage, M., Bundschuh, J., 2017. Antimony as a global dilemma: Geochemistry, mobility, fate and transport. *Environ. Pollut.* 223, 545–559. <http://dx.doi.org/10.1016/j.envpol.2017.01.057>

Ilacqua, V., Freeman, N.C.J., Fagliano, J., Liroy, P.J., 2003. The historical record of air pollution as defined by attic dust. *Atmos. Environ.* 37, 2379–2389. [https://doi.org/10.1016/S1352-2310\(03\)00126-2](https://doi.org/10.1016/S1352-2310(03)00126-2)

Jabłońska, M., Janeczek, J., 2019. Identification of industrial point sources of airborne dust particles in an urban environment by a combined mineralogical and meteorologic analyses: A case study from the Upper Silesian conurbation, Poland. *Atmos. Pollut. Res.* 10, 980–988. <https://doi.org/10.1016/j.apr.2019.01.006>

Jeong, C.H., Traub, A., Huang, A., Hilker, N., Wang, J.M., Herod, D., Dabek-Zlotorzynska, Celo, V., Evans, G.J., 2020. Long-term analysis of PM<sub>2.5</sub> from 2004 to 2017 in Toronto: Composition, sources, and oxidative potential. *Environ. Pollut.* 263, Part B, 114652. <https://doi.org/10.1016/j.envpol.2020.114652>

Karagulian, F., Belis, C.A., Dora, C.F.C., Prüss-Ustün, A.M., Bonjour, S., Adair-Rohani, H., Amann, M., 2015. Contributions to cities' ambient particulate matter (PM): A systematic review of local source contributions at global level. *Atmos. Environ.* 120, 475–483. <https://doi.org/10.1016/j.atmosenv.2015.08.087>

Kelepertzis, E., Chrastný, V., Botsou, F., Sigala, E., Kyritidou, Z., Komárek, M., Skordas, K., Argyraki, A., 2021. Tracing the sources of bioaccessible metal(loid)s in urban environments: A multidisciplinary approach. *Sci. Total Environ.* 771, 13 pp. <https://doi.org/10.1016/j.scitotenv.2020.144827>

Kiela, P.R., Ghishan, F.K., 2016. Physiology of Intestinal Absorption and Secretion. *Best Pract. Res. Clin. Gastroenterol.* 30, 145–159. <https://doi.org/10.1016/j.bpg.2016.02.007>

Lead Reach Consortium, 2012. Slags, lead reveratory smelting. International Lead Association. <https://ila-reach.org/wp-content/uploads/2016/07/Slags-lead-reveratory-smelting.pdf> Accessed April 2, 2021.

Lewis, S.L., Maslin, M.A., 2015. Defining the Anthropocene. *Nature* 519, 171–180. <https://doi.org/10.1038/nature14258>

Lyons, W.B., Harmon, R.S., 2012. Why urban geochemistry? *Elements* 8, 417–422. <https://doi.org/10.2113/gselements.8.6.417>

Marinho-Reis, A.P., Costa, C., Rocha, F., Cave, M., Wragg, J., Valente, T., Sequeira-Braga, A., Noack, Y., 2020. Biogeochemistry of Household Dust Samples Collected from Private Homes of a Portuguese Industrial City. *Geosciences* 10, 392. <https://doi.org/10.3390/geosciences10100392>

Mencin-Gale, E., Jamšek-Rupnik, P., Trajanova, M., Gale, L., Bavec, M., Anselmetti, F.S., Šmuc, A., 2019. Provenance and morphostratigraphy of the Pliocene-Quaternary sediments in the Celje and Drava-Ptuj Basins (eastern Slovenia). *Geologija* 62, 189–218. <https://doi.org/10.5474/geologija.2019.009>

Miler, M., 2014. SEM/EDS characterization of dusty deposits in precipitation and assessment of their origin. *Geologija* 57, 5–14. <https://doi.org/10.5474/geologija.2014.001>

Miler, M., 2020. Airborne particles in city bus: concentrations, sources and simulated pulmonary solubility. *Environ. Geochem. Health*. <https://doi.org/10.1007/s10653-020-00770-5> (online first)

Miler, M., Gosar, M., 2013. Assessment of Metal Pollution Sources by SEM/EDS Analysis of Solid Particles in Snow: A Case Study of Žerjav, Slovenia. *Microsc. Microanal.* 19, 1606–1619. <https://doi.org/10.1017/S1431927613013202>

Miler, M., Gosar, M., 2015. Chemical and morphological characteristics of solid metal-bearing phases deposited in snow and stream sediment as indicators of their origin. *Environ. Sci. Pollut. Res.* 22, 1906–1918. <https://doi.org/10.1007/s11356-014-3589-x>

Miler, M., Gosar, M., 2019. Assessment of contribution of metal pollution sources to attic and household dust in Pb- polluted area. *Indoor Air* 29, 487–498. <https://doi.org/10.1111/ina.12548>

Mioč, P., 1978. Basic Geological Map of SFR Yugoslavia 1:100.000, Explanatory Text for Slovenj Gradec Sheet. Zvezni geološki zavod. Beograd, 74 pp.

Mioč, P., Žnidarčič, M., 1989. Basic Geological Map of SFR Yugoslavia 1:100.000, Explanatory Text for Maribor and Leibnitz Sheet. Zvezni geološki zavod. Beograd, 60 pp.

Mitra, A., Sen, I.S., 2017. Anthrobiogeochemical platinum, palladium and rhodium cycles of earth: Emerging environmental contamination. *Geochim. Cosmochim. Acta* 216, 417–432. <https://doi.org/10.1016/j.gca.2017.08.025>

Nadbath, M., 2019. Meteorological station Maribor Tabor. Naše okolje-Mesečni bilten Agencije RS za okolje 26 (5), 56–69. <https://www.arso.gov.si/o%20agenciji/knji%C5%BEnica/mese%C4%8Dni%20bilten/NASE%20OKOLJE%20-%20Maj%202019.pdf>

Nalbandian, H., 2012. Trace element emissions from coal. IEA Clean Coal Centre, UK 89 pp. [https://usea.org/sites/default/files/092012\\_Trace%20element%20emissions%20from%20coal\\_ccc203.pdf](https://usea.org/sites/default/files/092012_Trace%20element%20emissions%20from%20coal_ccc203.pdf) Accessed April 9, 2021.

Oset, Ž., Berberih Slana, A., Lazarević, Ž. (Eds.), 2010. Mesto in gospodarstvo-Mariborsko gospodarstvo v 20. stoletju. Inštitut za novejšo zgodovino in Muzej narodne osvoboditve, Maribor, 616 pp. (In Slovene)

O'Shea, M.J., Vann, D.R., Hwang, W.T., Gieré, R., 2020. A Mineralogical and Chemical Investigation of Road Dust in Philadelphia, PA, USA. *Environ. Sci. Pollut. Res.* 27, 14883–14902. <https://doi.org/10.1007/s11356-019-06746-y>

Pacyna, J.M., Pacyna, E.G., 2001. An assessment of global and regional emissions of trace metals to the atmosphere from anthropogenic sources worldwide. *Environ. Rev.* 9, 269–298. <https://doi.org/10.1139/a01-012>

Painecur, P., Muñoz, A., Tume, P., Melipichun, T., Ferraro, F.X., Roca, N., Bech, J., 2022. Distribution of potentially harmful elements in attic dust from the City of Coronel (Chile). *Environ. Geochem. Health*, 10 pp. <https://doi.org/10.1007/s10653-021-01164-x>

Qin, J., Nworie, O.E., Lin, C., 2016. Particle size effects on bioaccessible amounts of ingestible soil-borne toxic elements. *Chemosphere* 159, 442–448. <http://dx.doi.org/10.1016/j.chemosphere.2016.06.034>

Rauch, J.N., Pacyna, J.M., 2009. Earth's global Ag, Al, Cr, Cu, Fe, Ni, Pb, and Zn cycles. *Global Biogeochemical Cycles* 23, 1–16. <https://doi.org/10.1029/2008GB003376>

Rode, B., 2009. Emissions of sulphur dioxide. Slovenian Environment Agency. <http://kazalci.arso.gov.si/sl/content/izpusti-zveplovega-dioksida-zadnji-podatki-na-voljo-v-sklopu-kazalca-zr09> Accessed April 13, 2021

Ruby, M.V., Davis, A., Schoof, R., Eberle, S., Sellstone, C.M., 1996. Estimation of lead and arsenic bioavailability using a physiologically based extraction test. *Environ. Sci. Technol.* 30, 422–430. <https://doi.org/10.1021/es950057z>

Šajn, R., 1999. Geochemical properties of urban sediments on the territory of Slovenia. *Geološki zavod Slovenije*, 136 pp.

Šajn, R., 2003. Distribution of chemical elements in attic dust and soil as reflection of lithology and anthropogenic influence in Slovenia. *Journal de Physique IV* 107, 1173–1176. <https://doi.org/10.1051/jp4:20030509>

Selin, N.E., 2009. Global Biogeochemical Cycling of Mercury: A Review. *Annual Review of Environment and Resources* 34, 43–63. <https://doi.org/10.1146/annurev.environ.051308.084314>

Slavec, A., 1991. Razvoj industrije v Mariboru s posebnim poudarkom na razvojnih dejavnikih. 8. Dela – Oddelek za geografijo Filozofske fakultete v Ljubljani, št.pp. 53–64. (In Slovene). <https://doi.org/10.4312/dela.8.53-64>

Slezakova, K., Pires, J.C.M., Pereira, M.C., Martins, F.G., Alvim-Ferraz, M.C., 2008. Influence of traffic emissions on the composition of atmospheric particles of different sizes – Part 2: SEM-EDS characterization. *J. Atmos. Chem.* 60, 221–236. <https://doi.org/10.1007/s10874-008-9117-y>

Sokol, E.V., Kalugin, V.M., Nigmatulina, E.N., Volkova, N.I., Frenkel, A.E., Maksimova, N.V., 2002. Ferrospheres from fly ashes of Chelyabinsk coals: chemical composition, morphology and formation conditions. *Fuel* 81, 867–876. [https://doi.org/10.1016/S0016-2361\(02\)00005-4](https://doi.org/10.1016/S0016-2361(02)00005-4)

Šoster, A., Zavašnik, J., Ravnjak, M., Herlec, U., 2017. REE-bearing minerals in Drava river sediments, Slovenia, and their potential origin. *Geologija* 60, 257–266. <https://doi.org/10.5474/geologija.2017.018>

Tack, F.M.G., 2010. Trace elements: General Soil Chemistry, Principles and Processes. In: Hooda, P. S. (ed.). 2010. Trace elements in soils. Wiley, UK, 9–37.

Talovskaya, A.V., Yazikov, E.G., Filimonenko, E.A., Lata, J.C., Kim, J., Shakhova, T.S., 2017. Characterization of solid airborne particles deposited in snow in the vicinity of urban fossil fuel thermal power plant (Western Siberia). *Environ. Technol.* 39, 2288–2303. <https://doi.org/10.1080/09593330.2017.1354075>

Teran, K., Žibret, G., Fanetti, M., 2020. Impact of urbanization and steel mill emissions on elemental composition of street dust and corresponding particle characterization. *J. Hazard. Mater.* 384. <https://doi.org/10.1016/j.jhazmat.2019.120963>

Thorpe, A., Harrison, R.M., 2008. Sources and properties of non-exhaust particulate matter from road traffic: A review. *Sci. Total Environ.* 400, 270–282. <https://doi.org/10.1016/j.scitotenv.2008.06.007>

Tye, A.M., Hodgkinson, E.S., Rawlins, B.G., 2006. Microscopic and chemical studies of metal particulates in tree bark and attic dust: evidence for historical atmospheric smelter emissions, Humberside, UK. *J. Environ. Monit.* 8, 904–912. <https://doi.org/10.1039/B605729B>

Umbria, A., Galán, M., Muñoz, M. J., Martín, R., 2004. Characterization of atmospheric particles: analysis of particles in the Campo de Gibraltar. *Atmósfera*, 17, 191–206. [http://www.scielo.org.mx/scielo.php?script=sci\\_arttext&pid=S0187-62362004000400001](http://www.scielo.org.mx/scielo.php?script=sci_arttext&pid=S0187-62362004000400001)

USEPA, 2008. Guidance for the sampling and analysis of lead in indoor residential dust for use in the integrated exposure uptake biokinetic (IEUBK) model. United States Environmental Protection Agency, Office of superfund remediation and technology innovation, Technical review workgroup for metals and asbestos, Lead committee, 21 pp.

Van Alphen, M., 1998. Paint Film Components. National Environmental Health Forum Monographs, General Series No. 2, 113–117.

Van Pelt, R.S., Shekhter, E.G., Barnes, M.A.W., Duke, S.E., Gill, T.E., Pannell, K.H., 2020. Spatial and temporal patterns of heavy metal deposition resulting from a smelter in El Paso, Texas. *J. Geochem. Explor.* 210, 1–8. <https://doi.org/10.1016/j.gexplo.2019.106414>

Vítková, M., Ettler, V., Šebek, O., Mihaljevič, M., Grygar, T., Rohovec, J., 2009. The pH-dependent leaching of inorganic contaminants from secondary lead smelter fly ash. *J. Hazard. Mater.* 167, 427–433. <https://doi.org/10.1016/j.jhazmat.2008.12.136>

Völgyesi, P., Jordan, G., Zacháry, D., Szabó, C., Bartha, A., Matschullat, J., 2014. Attic dust reflects long-term airborne contamination of an industrial area: A case study from Ajka, Hungary. *Appl. Geochemistry* 46, 19–29. <https://doi.org/10.1016/j.apgeochem.2014.03.010>

Wheeler, A.J., Jones, P.J., Reisen, F., Melody, S.M., Williamson, G., Strandberg, B., Hinwood, A., Almerud, P., Blizzard, L., Chappell, K., Fisher, G., Torre, P., Zosky, G.R., Cope, M., Johnston, F.H., 2020. Roof cavity dust as an exposure proxy for extreme air pollution events. *Chemosphere* 244, 1–9. <https://doi.org/10.1016/j.chemosphere.2019.125537>

Wong, C.S.C., Li, X., Thornton, I., 2006. Urban environmental geochemistry of trace metals. *Environ. Pollut.* 142, 1–16. <https://doi.org/10.1016/j.envpol.2005.09.004>

Wragg, J., Cave, M., Taylor, H., Basta, N., Brandon, E., Casteel, S., Gron, C., Oomen, A., Van de Wiele, T., 2009. Interlaboratory Trial of a Unified Bioaccessibility Procedure. British Geological Survey, Open Report OR/07/027. <https://nora.nerc.ac.uk/id/eprint/7491/1/OR07027.pdf>

Wragg, J., Cave, M., Basta, N., Brandon, E., Casteel, S., Denys, S., Gron, C., Oomen, A., Reimer, K., Tack, K., Van de Wiele, T., 2011. An inter-laboratory trial of the unified BARGE bioaccessibility method for arsenic, cadmium and lead in soil. *Sci. Total Environ.* 409, 4016–4030. <https://doi.org/10.1016/j.scitotenv.2011.05.019>

Yongming, H., Peixuan, D., Junji, C., Posmentier, W.S., 2006. Multivariate analysis of heavy metal contamination in urban dusts of Xi'an, Central China. *Sci. Total Environ.* 355, 176–186. <https://doi.org/10.1016/j.scitotenv.2005.02.026>

Žibret, G., 2008. Determination of historical emission of heavy metals into the atmosphere: Celje case study. *Environ. Geol.* 56, 189–196. <https://doi.org/10.1007/s00254-007-1151-6>

Žibret, G., 2018. Influences of coal mines, metallurgical plants, urbanization and lithology on the elemental composition of street dust. *Environ. Geochem. Health* 41, 1489–1505. <https://doi.org/10.1007/s10653-018-0228-3>

Žibret, G., Van Tonder, D., Žibret, L., 2013. Metal content in street dust as a reflection of atmospheric dust emissions from coal power plants, metal smelters, and traffic. *Environ. Sci. Pollut. Res.* 20, 4455–4468. <https://doi.org/10.1007/s11356-012-1398-7>

Zupančič, M., Šušteršič, M., Bavec, Š., Gosar, M., 2021. Oral and inhalation bioaccessibility of potentially toxic elements in household dust from former Hg mining district, Idrija, Slovenia. *Environ. Geochem. Health* 43, 3505–3531. <https://doi.org/10.1007/s10653-021-00835-z>

**Figure captions:** (in colour on the Web only; all figures are 2-column images)

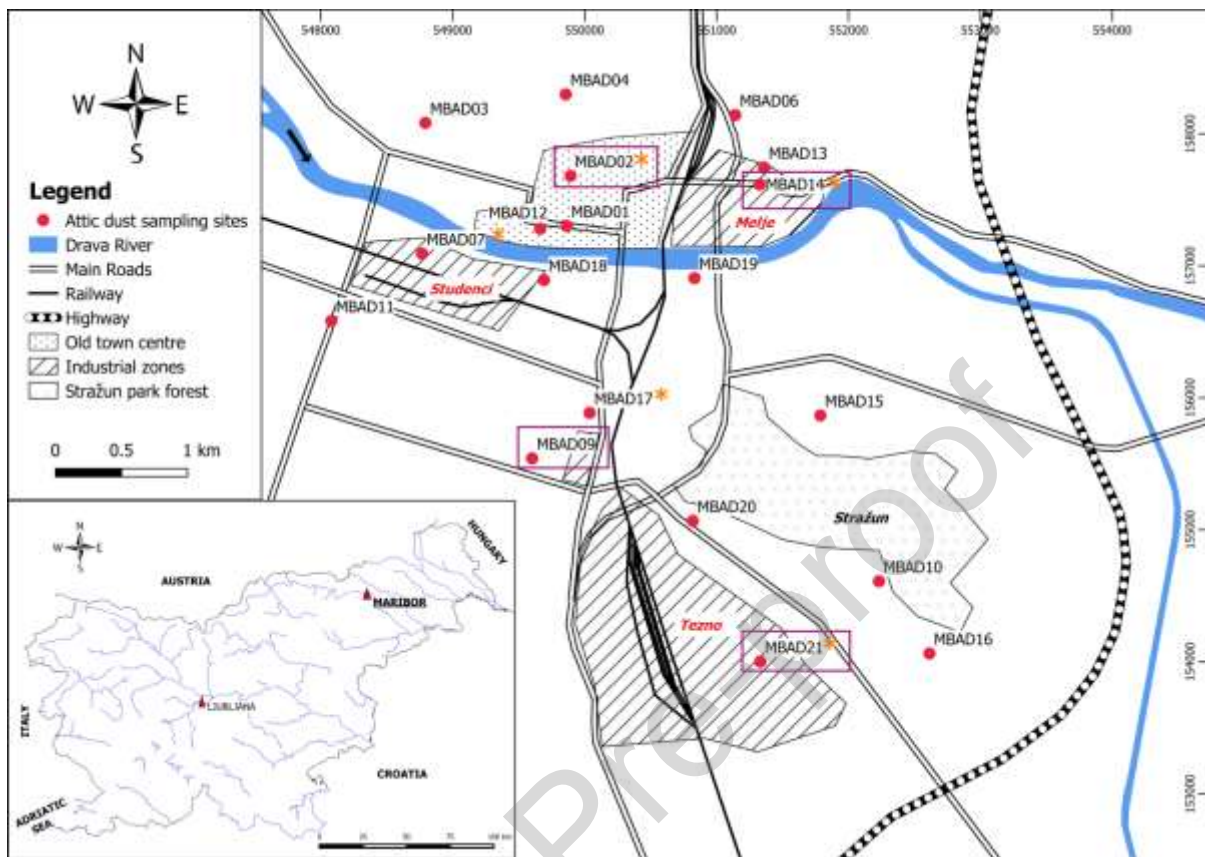


**Fig. 1:** Attic dust sampling sites on schematic map of Maribor (four framed samples were analysed with SEM/EDS and oral bioaccessibility (UBM) was analysed in five samples marked with an orange asterisk).

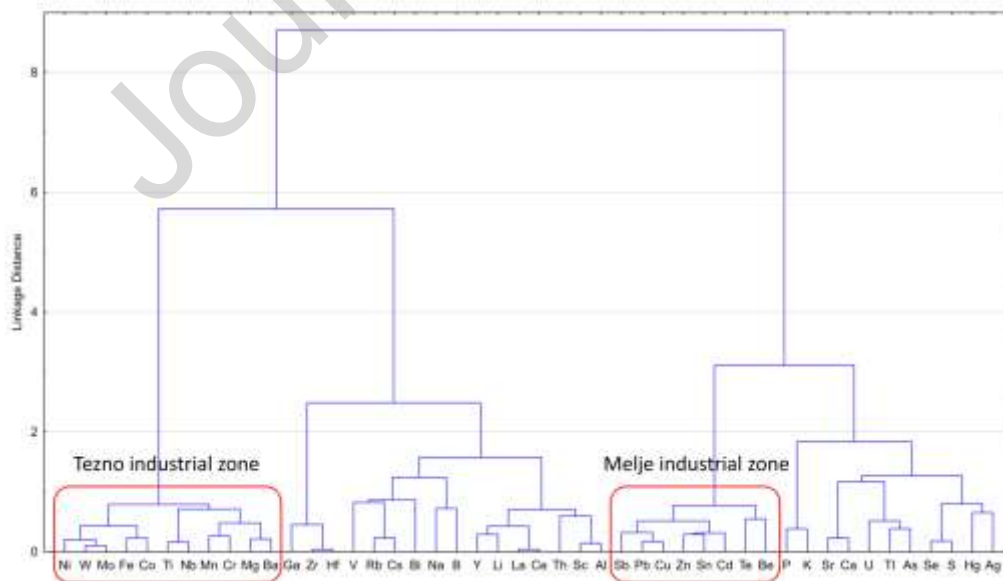


**Fig. 2:** Dendrogram of chemical elements in attic dust samples.

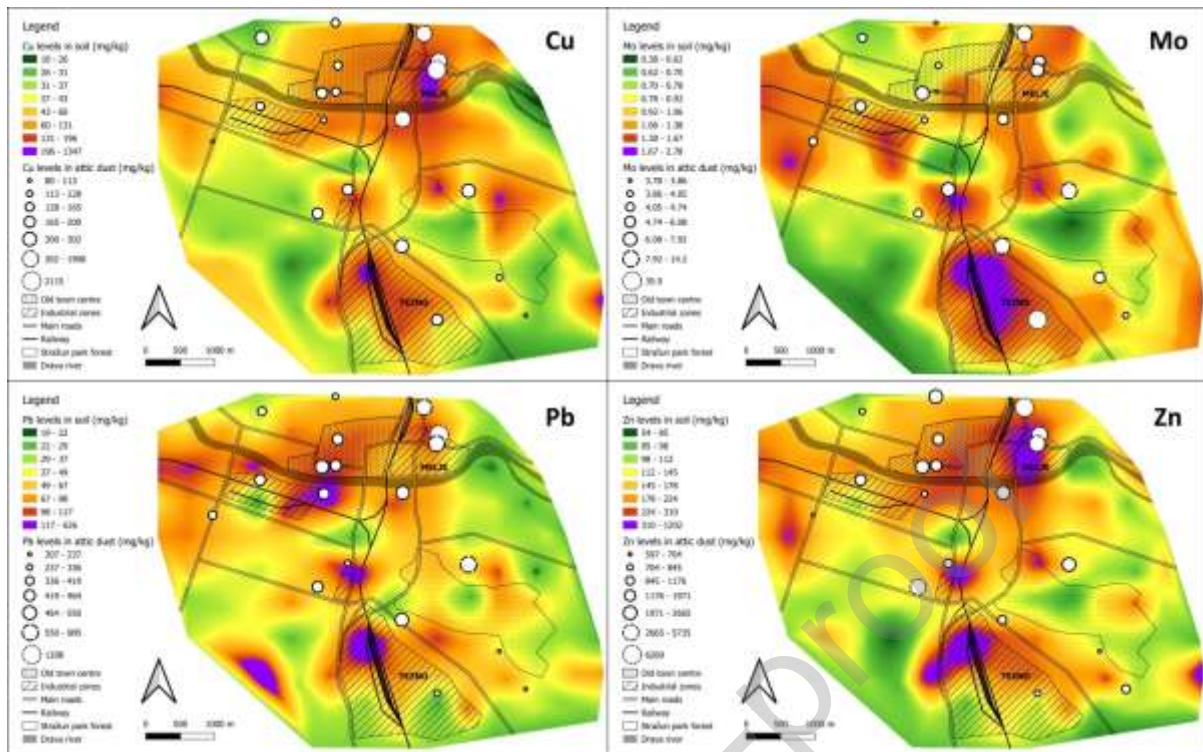


**Fig. 3:** Spatial distribution of Cu, Mo, Pb and Zn in attic dust (graduated circles) given on interpolated soil maps (soil data taken from Gaberšek & Gosar, 2018).

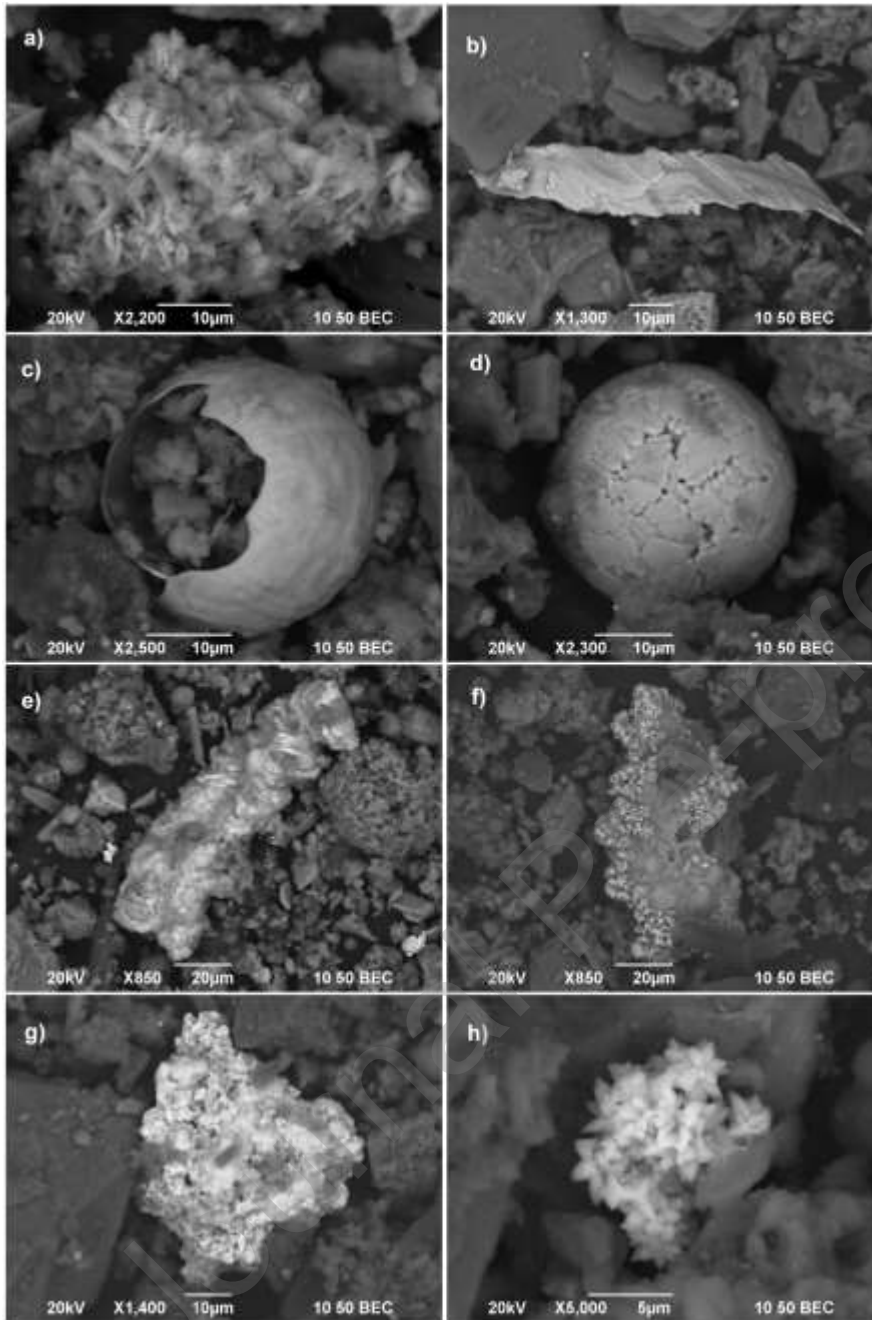


**Fig. 4:** SEM images of (a) Ca-S-O (gypsum) particle (MBAD09); (b) thin sharp-edged shaving of Fe-O (MBAD21-Tezno); (c) hollow Fe-O sphere (MBAD21-Tezno); (d) skeletal-dendritic Fe-O (Mn, Cr) sphere (MBAD21-Tezno); (e) elongated shaving of Cu-Zn (Cl) (MBAD14-Melje); (f) irregularly shaped particle Cu-Zn-Cl (darker area in the middle) with Cu-S-Cl crystals on its surface (bright areas) that were probably formed *in-situ* by the reaction of particles with atmospheric SO<sub>2</sub>; (g) Pb-S-O (Cu, Zn) particle, possible mineral anglesite (MBAD14-Melje); (h) K-Pb-S-O (Cu, Zn) particle, possibly anthropogenically-derived mineral palmierite (MBAD14-Melje).

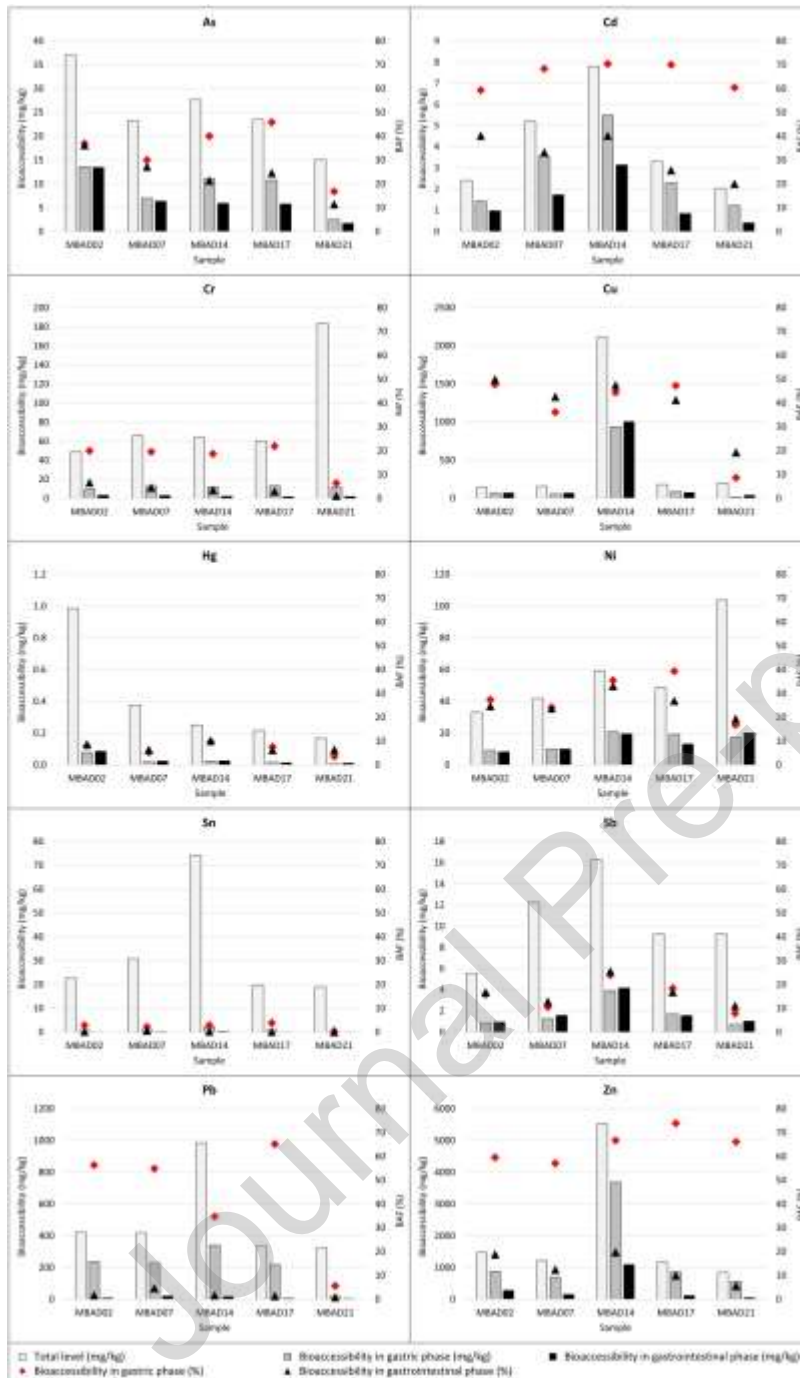


**Fig. 5:** Oral bioaccessibility of As, Cd, Cr, Cu, Hg, Ni, Pb, Sb, Sn, and Zn in gastric and gastrointestinal phases of all five analysed samples, given in mg/kg (columns) and % (triangles and rhombuses); total levels are also given (in mg/kg; columns).

**Table captions:**

**Table 1:** Descriptive statistics of chemical analyses of attic dust (levels are given in mg/kg, except for Al, Ca, Fe, K, Mg, Na, P, S, Ti, and TOC, which are given in %; N = 19) and normalised enrichment factors (EF) for elements in attic dust according to their soil medians.

	Min <sup>1</sup>	P25	X	Md <sup>1</sup>	Xg	P75	Max <sup>1</sup>	A	E	EF
Ag	0.38	0.50	0.68	0.66	0.64	0.81	1.22	0.88	0.59	10.1
Al	0.96	1.10	1.21	1.16	1.20	1.37	1.52	0.50	-0.64	(1)
As	13	19	25	24	23	26	52	1.97	5.83	3.3
B	10	20	38	25	25	29	290	4.18	17.89	8.8
Ba	54	101	114	109	109	120	198	0.70	1.57	1.6
Be	0.3	0.5	0.6	0.6	0.6	0.7	0.9	0.24	-0.23	1.2
Bi	1.1	1.5	1.9	1.8	1.8	2.2	3.1	0.65	0.20	8.9
Ca	4.4	5.7	6.6	6.4	6.5	7.4	9.2	0.56	-0.04	8.1
Cd	1.6	2.4	3.5	3.0	3.2	4.9	7.8	1.36	1.07	13
Ce	18	19	22	20	21	23	34	1.96	4.74	1.0
Co	5.8	7.2	9.2	8.9	8.9	9.9	18.6	2.25	6.74	1.2
Cr	40	51	68	61	64	66	184	2.95	10.06	2.8
Cs	1.4	1.7	1.9	1.8	1.9	2.2	3.0	1.29	2.35	1.7
Cu	80	128	422	193	250	302	2115	2.45	5.15	6.8
Dy	1.4	1.5	1.7	1.6	1.7	1.8	2.2	0.91	-0.12	1.2
Er	0.67	0.75	0.89	0.88	0.88	0.93	1.17	0.44	-0.40	1.3
Eu	0.35	0.43	0.50	0.48	0.49	0.53	0.76	1.33	1.90	1.2
Fe	1.79	2.03	2.43	2.30	2.37	2.60	4.28	1.85	3.72	1.3
Ga	4.6	5.4	5.8	5.6	5.8	6.2	7.5	0.77	0.77	1.8
Gd	1.5	1.6	1.9	1.9	1.9	2.1	3.0	1.28	1.78	1.2
Hg	0.17	0.25	0.60	0.32	0.39	0.44	4.65	4.07	17.14	4.7
Ho	0.27	0.30	0.35	0.34	0.34	0.37	0.49	1.10	1.06	1.5
K	0.22	0.25	0.32	0.29	0.30	0.35	0.54	1.22	0.89	3.3
La	9.6	10	12	11	12	13	23	2.47	7.37	1.1
Li	15	16	19	18	19	22	28	0.98	0.08	1.4
Lu	0.09	0.09	0.11	0.11	0.11	0.13	0.15	0.75	-0.74	1.5
Mg	0.79	1.09	1.34	1.30	1.29	1.48	2.59	1.53	4.00	2.3
Mn	332	425	495	474	485	573	754	0.81	0.66	1.1
Mo	3.8	4.1	7.5	5.5	6.1	7.9	36	3.63	14.15	9.1
Na	0.07	0.10	0.12	0.11	0.12	0.15	0.20	0.54	0.14	16
Nb	1.4	1.8	2.1	2.1	2.1	2.3	3.0	0.51	-0.56	4.2
Nd	7.7	7.9	9.6	8.8	9.4	10.6	17.5	2.23	5.97	1.0
Ni	25	36	50	42	47	59	104	1.34	1.29	2.1
P	0.098	0.118	0.159	0.137	0.148	0.164	0.446	3.00	10.55	2.1
Pb	207	336	500	424	454	550	1208	1.67	2.99	14
Pr	2.0	2.3	2.7	2.5	2.7	2.9	5.1	2.49	7.72	1.1
Rb	18	19	22	21	22	25	38	1.48	1.67	1.5
S	1.93	3.52	4.10	4.17	3.92	4.76	6.90	0.38	0.71	147
Sb	4.9	5.9	9.0	9.3	8.4	12	16	0.57	-0.77	15
Sc	1.7	3.0	3.2	3.2	3.1	3.5	3.9	-1.66	5.60	1.4
Se	0.6	1.6	1.9	1.9	1.8	2.3	2.8	-0.40	0.74	6.7

<b>Sm</b>	1.6	1.6	1.9	1.9	1.9	2.2	2.9	1.32	1.60	1.1
<b>Sn</b>	15	20	29	23	26	31	74	1.96	3.57	14
<b>Sr</b>	99	114	132	126	129	141	213	1.67	3.15	8.9
<b>Tb</b>	0.24	0.26	0.31	0.31	0.30	0.34	0.45	0.87	0.49	1.3
<b>Te</b>	0.03	0.05	0.06	0.06	0.06	0.07	0.12	1.25	3.55	/
<b>Th</b>	0.40	2.1	2.3	2.3	2.1	2.5	2.9	-2.58	9.27	1.6
<b>Ti</b>	0.028	0.042	0.053	0.052	0.051	0.063	0.078	0.14	-0.67	2.8
<b>Tl</b>	0.18	0.24	0.27	0.27	0.27	0.30	0.33	-0.59	0.13	2.2
<b>Tm</b>	0.09	0.11	0.12	0.12	0.12	0.13	0.17	0.77	0.55	1.4
<b>U</b>	1.4	1.9	2.5	2.4	2.4	2.9	3.8	0.35	-0.82	3.1
<b>V</b>	50	61	73	69	71	83	95	0.10	-1.06	3.0
<b>W</b>	1.3	1.7	4.8	2.6	2.9	3.6	41	4.23	18.19	/
<b>Y</b>	7.1	8.0	9.0	8.9	8.9	9.3	12.5	1.27	2.04	1.4
<b>Yb</b>	0.57	0.67	0.75	0.74	0.74	0.79	0.91	0.28	-0.46	1.3
<b>Zn</b>	597	845	2171	1478	1658	2665	6269	1.47	1.07	16
<b>Zr</b>	1.2	4.1	5.2	5.4	4.8	6.4	9.2	-0.23	1.01	25
<b>TOC<sup>2</sup></b>	5.0	5.1	6.3	5.9	6.2	7.1	9.4	1.11	0.69	2.7

<sup>1</sup>Gaberšek & Gosar, 2021; <sup>2</sup>TOC was analysed for only 12 samples; Min – minimum level; P25 – 25th percentile (Q1); X – mean; Md – median; Xg – geometric mean; P75 – 75th percentile (Q3); Max – maximum level; A – skewness; E – kurtosis; EF – Al-normalised enrichment factor according to soil medians.

**Table 2:** Assessed proportions of minerals and other phases (in %) in four attic dust samples and their means.

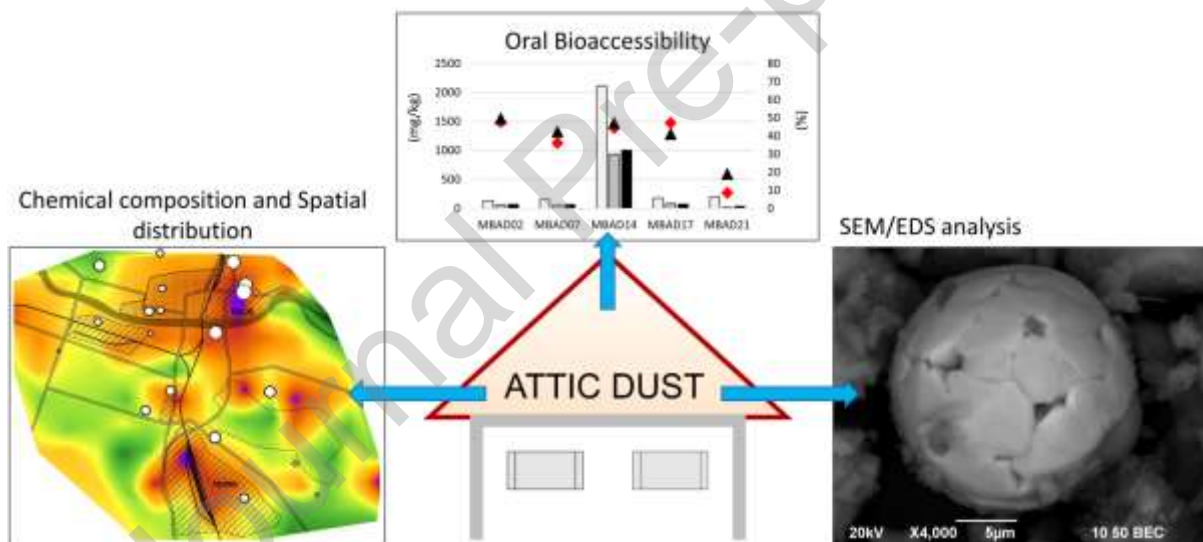
	<b>MBAD02</b>	<b>MBAD09</b>	<b>MBAD14</b>	<b>MBAD21</b>	<b>MEAN</b>
<b>CARBONATES</b>	<b>3.4</b>	<b>9.0</b>	<b>3.6</b>	<b>16</b>	<b>8.1</b>
➤ dolomite	2.8	3.4	3.2	13	5.6
➤ calcite	0.6	5.6	0.4	3.4	2.5
<b>SILICATES</b>	<b>30</b>	<b>35</b>	<b>31</b>	<b>35</b>	<b>33</b>
➤ quartz	16	15	15	18	16.2
➤ Al-silicates:	14	20	16	17	16.7
• <i>K-feldspar</i>	8.3	7.1	11.1	9.5	9.0
• <i>Na-feldspar</i>	2.8	6.5	4.1	4.7	4.5
• <i>Other silicates</i>	2.4	6.1	1.0	3.0	3.1
<b>PTE-BEARING PARTICLES</b>	<b>2.6</b>	<b>2.9</b>	<b>3.7</b>	<b>12</b>	<b>5.3</b>
<b>C-RICH PARTICLES</b>	<b>5.0</b>	<b>11</b>	<b>10</b>	<b>7.0</b>	<b>8.3</b>
<b>GYPSUM</b>	<b>59</b>	<b>42</b>	<b>50</b>	<b>30</b>	<b>45</b>

**Table 3:** Proportions of groups of PTE-bearing particles (in %) and their mean sizes in  $\mu\text{m}$  (given in brackets).

	<b>MBAD02</b> (N = 260)	<b>MBAD09</b> (N = 318)	<b>MBAD14</b> (N = 280)	<b>MBAD21</b> (N = 436)	<b>TOTAL</b> (N = 1294) <sup>1</sup>
<b>Fe-oxides</b>	40	51	41	54	48 (4.2)
<b>Spherical Fe-oxides</b>	14	7.9	4.6	19	12 (3.5)
<b>Fe-alloys</b>	0.8	1.6	3.2	3.0	2.2 (14.1)
<b>Fe-silicates</b>	0.4	0	0.4	0.2	0.2 (16.7)
<b>Sulphates/Sulphides</b>	18	15	22	13	16 (3.0)
<b>Other metal oxides</b>	3.1	1.9	6.1	1.8	3.0 (3.1)
<b>Other metal alloys</b>	0	0	2.5	0	0.5 (18.2)
<b>Spherical Si-particles</b>	13	12	12	5.3	9.8 (4.8)
<b>Other particles</b>	12	11	7.9	4.6	8.4 (4.6)
<i>(Mean size)</i>	<i>(3.2)</i>	<i>(3.8)</i>	<i>(4.5)</i>	<i>(5.2)</i>	<i>(4.3)</i>

<sup>1</sup>Gaberšek & Gosar, 2021; N = number of analysed PTE-bearing particles

## Graphical abstract



**CRedit authorship contribution statement**

**Martin Gaberšek:** conceptualization, data curation, methodology, formal analysis, investigation, resources, writing - original draft, visualization. **Michael J. Watts:** methodology, writing - review & editing. **Mateja Gosar:** conceptualization, methodology, writing - review & editing, supervision.

Journal Pre-proof

**Statement of novelty**

The novelty of the presented research is that the entire life cycle of attic dust in urban area is addressed, including its hazard to human health. Although attic dust is usually considered only as a proxy for historical air contamination, high levels of potentially toxic elements, high oral bioaccessibility of some of them as well as the potential for long-term exposure, discussed in the paper, indicate that attic dust should be considered also as a hazardous material for human health. As such, it fits the aims and scope of the Journal of Hazardous Materials.

Journal Pre-proof

**Declaration of interests**

The authors declare that they have no known competing financial interests or personal relationships that could have appeared to influence the work reported in this paper.

The authors declare the following financial interests/personal relationships which may be considered as potential competing interests:

Journal Pre-proof

Highlights:

- Attic dust (AD) allows identification of past emission sources
- Comprehensive study of entire life cycle of AD in an urban area is presented
- Impact of diverse industrial activities was recognised
- High oral bioaccessibility of some elements indicates potential health hazard of AD

Journal Pre-proof